Infall towards massive star forming regions

Friedrich Wyrowski, Rolf Güsten, Karl Menten, Helmut Wiesemeyer & Bernd Klein

MPIfR Bonn

Outline

Infall is a fundamental process in SF!

- ATLASGAL
- Infall in MSFR
  - Blue skewed profiles
  - Inverse P-cygni
  - Redshifted abs.
    - Vla cm results
- Ammonia
- SOFIA observations
- The sample:
  - G31/G34/W43
- Results
- Modeling
- Cycle I outlook

High mass star formation:
The quest for an evolutionary scheme

- Pre-protocluster cores: cold (<20K), massive (~100-1000 M)
- Pre-hot cores: IRAS sources, with/without strong MIR. “Warm” sources, T~50K
- Hot cores: internally heated, T>100K, dense (~10^7), HII region quenched
- Hyper-/ultra-compact HII regions: d<0.05pc, EM~10^9 / d<0.1pc, EM~10^7
- (compact) HII regions
- Endproducts: OB clusters/associations
- → How to probe all early stages in an unbiased way? observable ?

ATLASGAL: APEX Telescope Large Area Survey of the Galaxy

- MPG/Germany:

  F. Schuller (PI, now @ APEX), T. Csengeri, K. Menten, **F. Wyrowski (MPIfR)**, H. Beuther, T. Henning, H. Linz, P. Schilke

- ESO countries:

  M. Walmsley (co-PI), S. Bontemps, R. Cesaroni, L. Deharveng, F. Herpin, B. Lefloch, S. Molinari, F. Motte, V. Minier, L.-A. Nyman, V. Reveret, C. Risacher, N. Schneider, L. Testi, A. Zavagno

- Chile: L. Bronfman (co-PI), G. Garay, D. Mardones

+ A growing number of students !

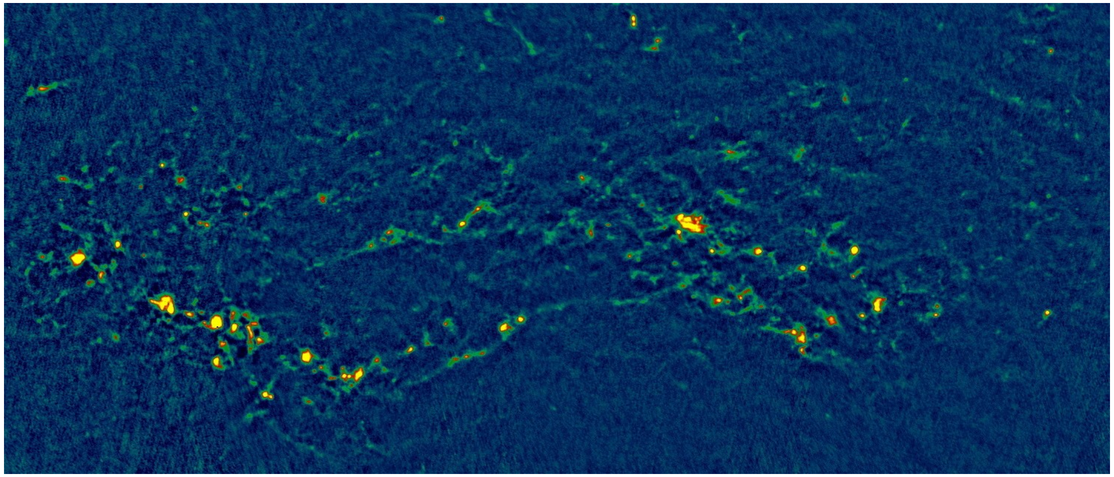

ATLASGAL (Schuller+2009):

- Unbiased survey of the inner Galactic Plane at 870µm
  - Census of massive star formation throughout the Galaxy
  - study large scale structure of the cold ISM
  - associate w. other Galactic surveys (VLA, Spitzer, MSX, Hi-GAL)
  - → evolutionary sequence of massive star forming clumps
- Main survey: mapping |l| < 60, |b| < 1.5
  - sensitivity 1σ = 50~mJy/beam
  - 3σ: 1 $M_\odot$ ~ at 500 pc, 35 $M_\odot$ ~ at 3 kpc, 240 $M_\odot$ ~ at 8 kpc
- Complementary to:
  - 1.1mm BGPS in the north
  - Herschel Hi-Gal Galactic plane survey

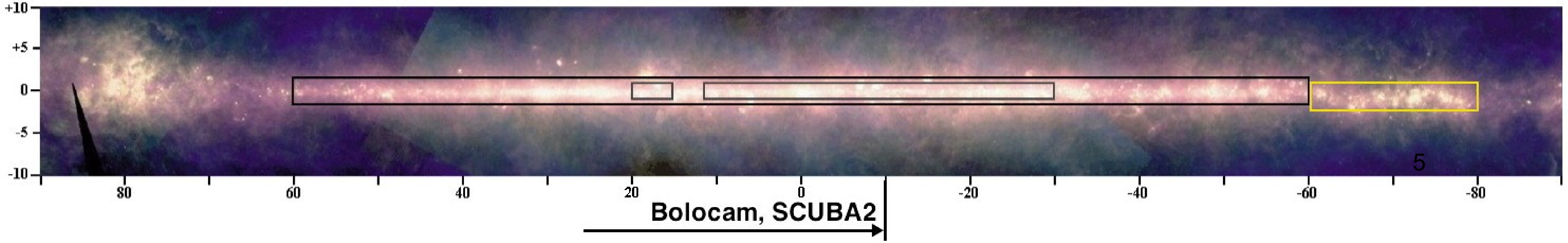

Example Norma arm: compact sources and long filaments

- Extended objects on arcmin scale
- Very long filaments, up to the degree scale!

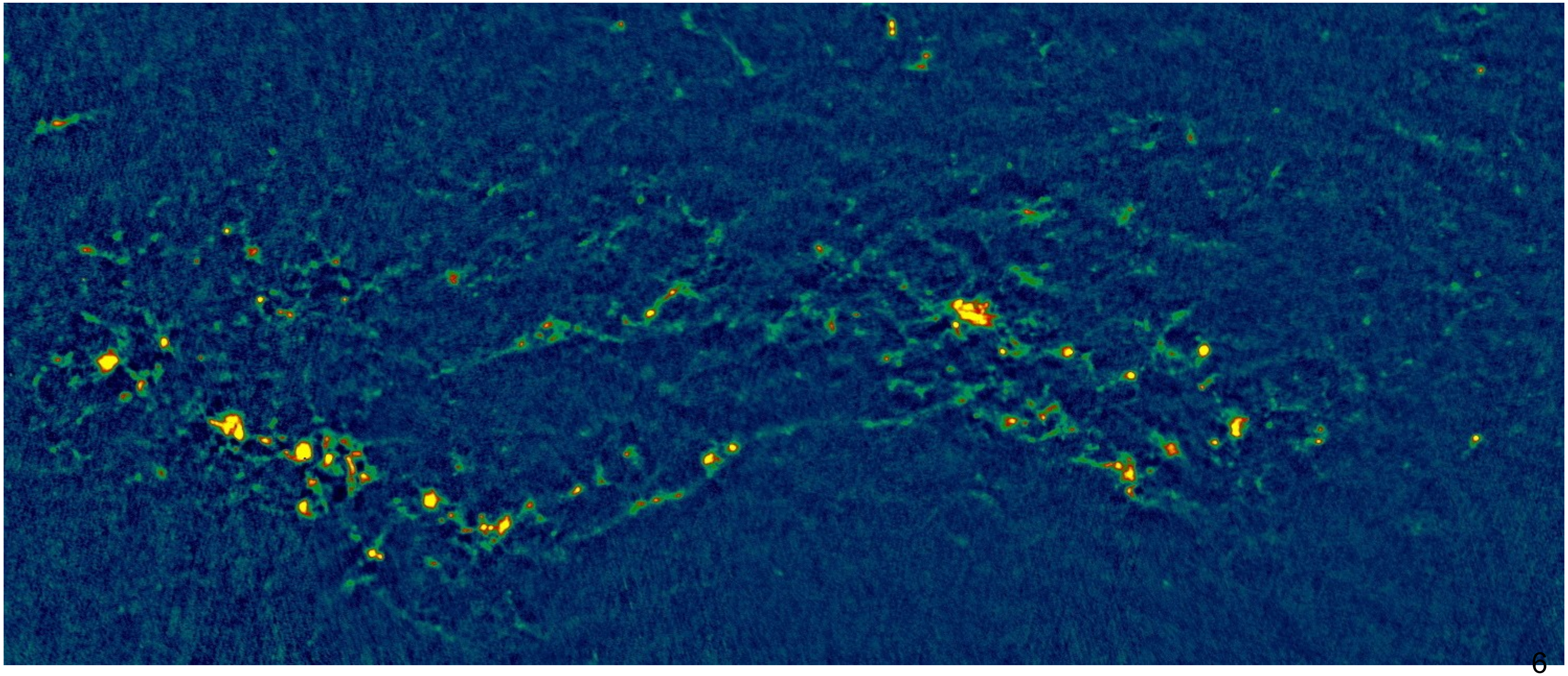

3 degrees cutout

Compact sources catalog in l=330-21: 6640 dust clumps Contreras+2012

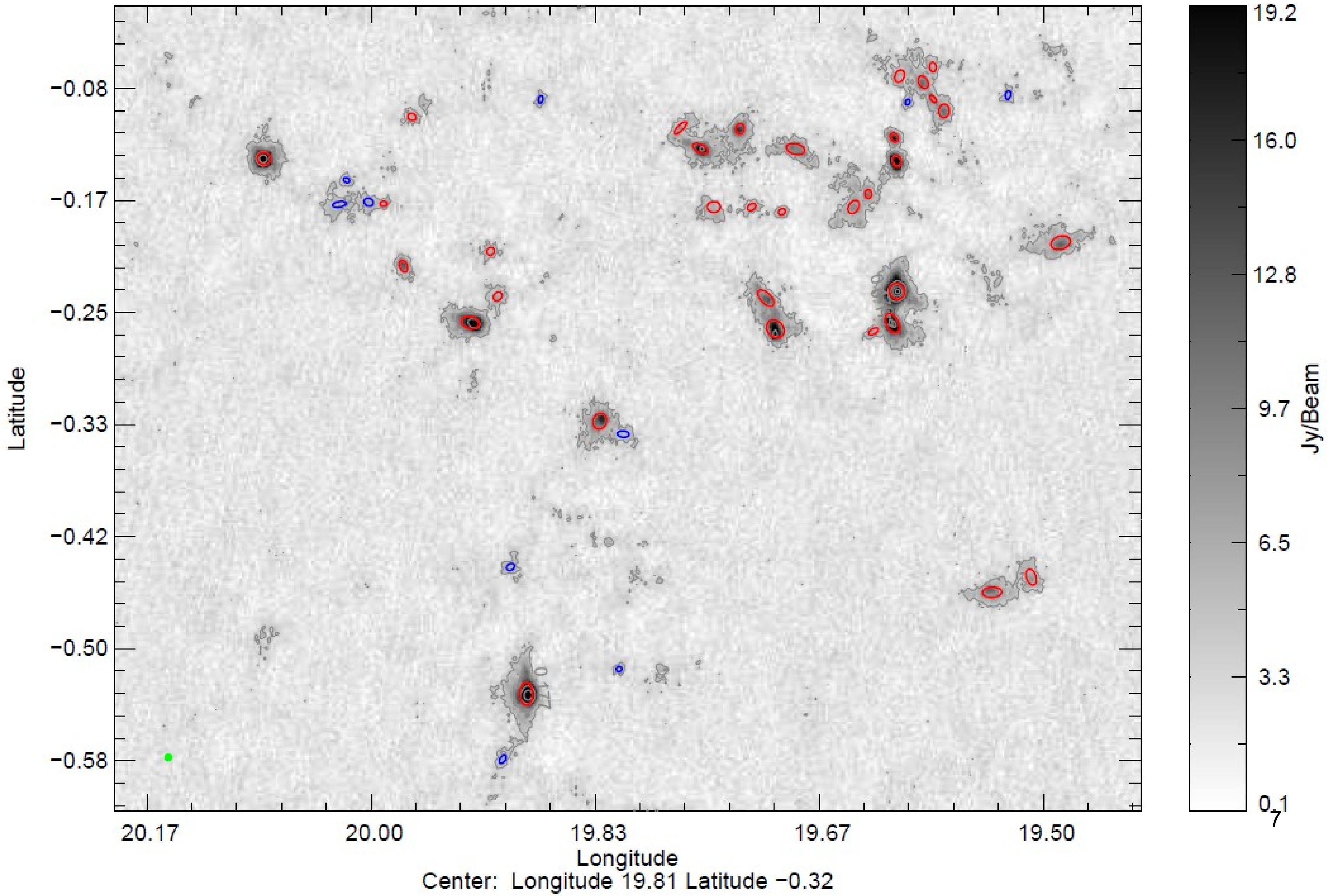

http://www3.mpifr-bonn.mpg.de/div/atlasgal/

(thanks to James Urquhart)

The ATLASGAL Database Server

ATLASGAL Summary Page: AGAL010.228-00.207

Dust Emission Image and Catalogue Parameters

ATLASGAL 870 µm Emission Map (5' x 5')

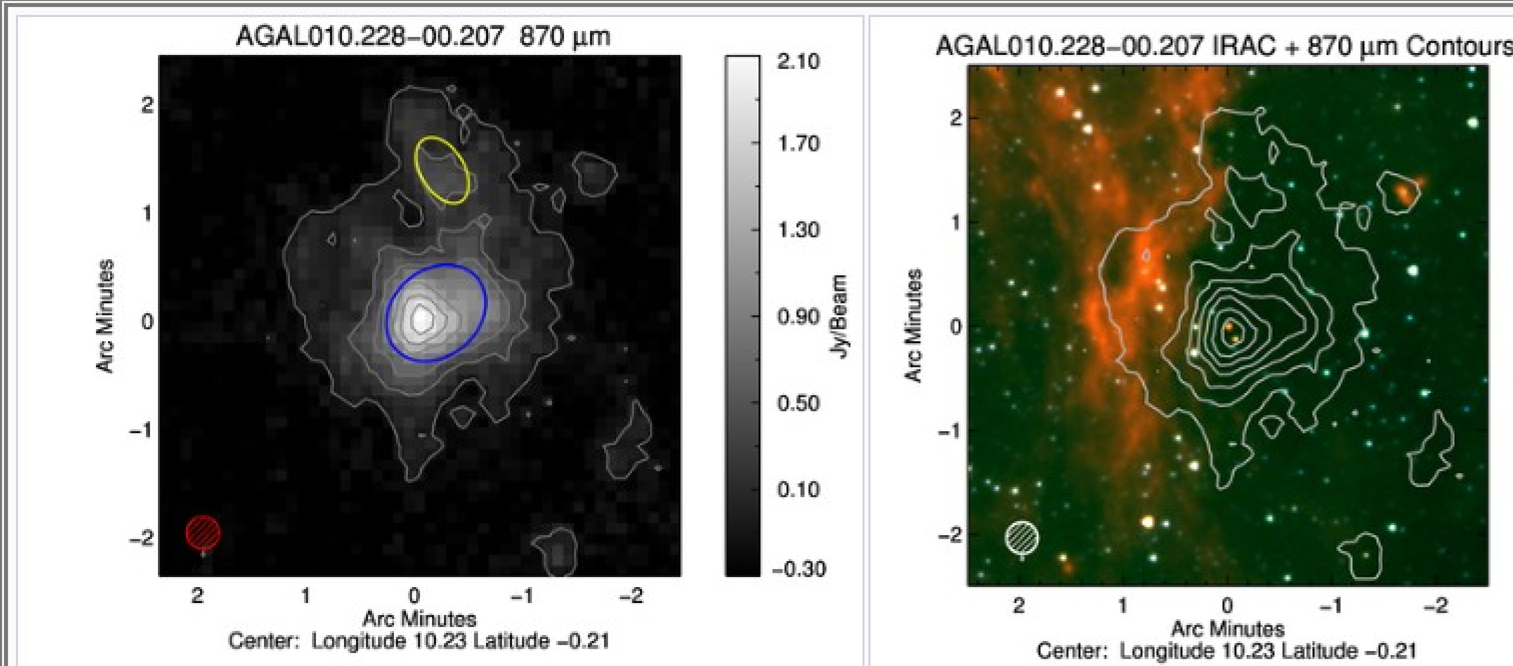

(fits file) (postscript file)

(3.5µm 4.6µm 5.8µm 8.0µm fits files) (postscript file)

Some statistics

- 6 % within 20” of Becker+1994 cm source
- Deharveng+2010: HII regions enclosed by bubbles
  - 40% surrounded by collected material
  - 28% interaction with dust condensations
  - Rest: uncertain or no association
- 71 % of MMBs within 20” of ATLASGAL peak, 96% associated with submm
- 50 % no IRAS/MSX
- 35 % associated with IRDCs radius of

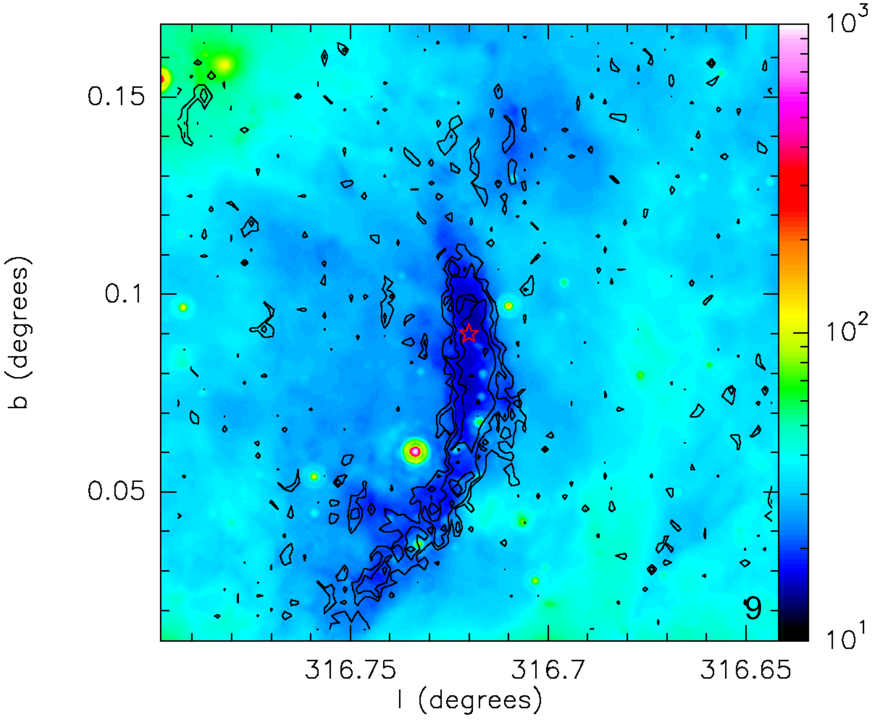

Molecular line follow ups

- Dust continuum is important but molecular line information is indispensable !
- Effelsberg/Parkes Ammonia (Wienen+2012, 2013):
  - Kinematic distances, temperatures
- IRAM 30m/ATNF-Mopra/APEX (Wyrowski/Csengeri):
  - 3 & 0.85mm line surveys: Physical & chemical conditions
- 30m/HERA IRAM large program: l=30 large scale molecular mapping (Motte+, Schilke+)
- MALT90 (Jackson+): Mopra Galactic Plane Survey of high density regions. large program:
  - → about 2000 ATLASGAL clumps mapped at 3mm
- Herschel/HIFI: 100 ATLASGAL sources currently observed in water lines → ATLASGAL water legacy (Wyrowski+)

APEX 345 GHz line surveys of bright ATLASGAL sources

- IR flux-limited samples:
  - 25 brightest ATLASGAL
  - 25 brightest MSX selected YSO
  - 25 brightest 8mu dark
  - 25 brightest 24mu dark
- → Select from all groups brightest objects for SOFIA follow ups !

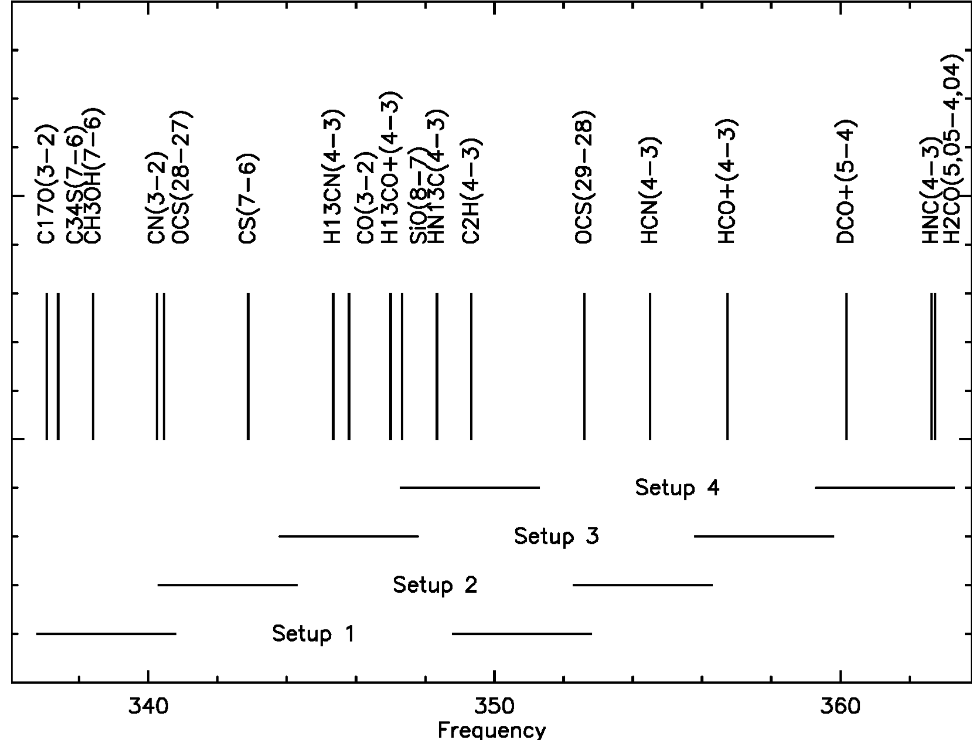

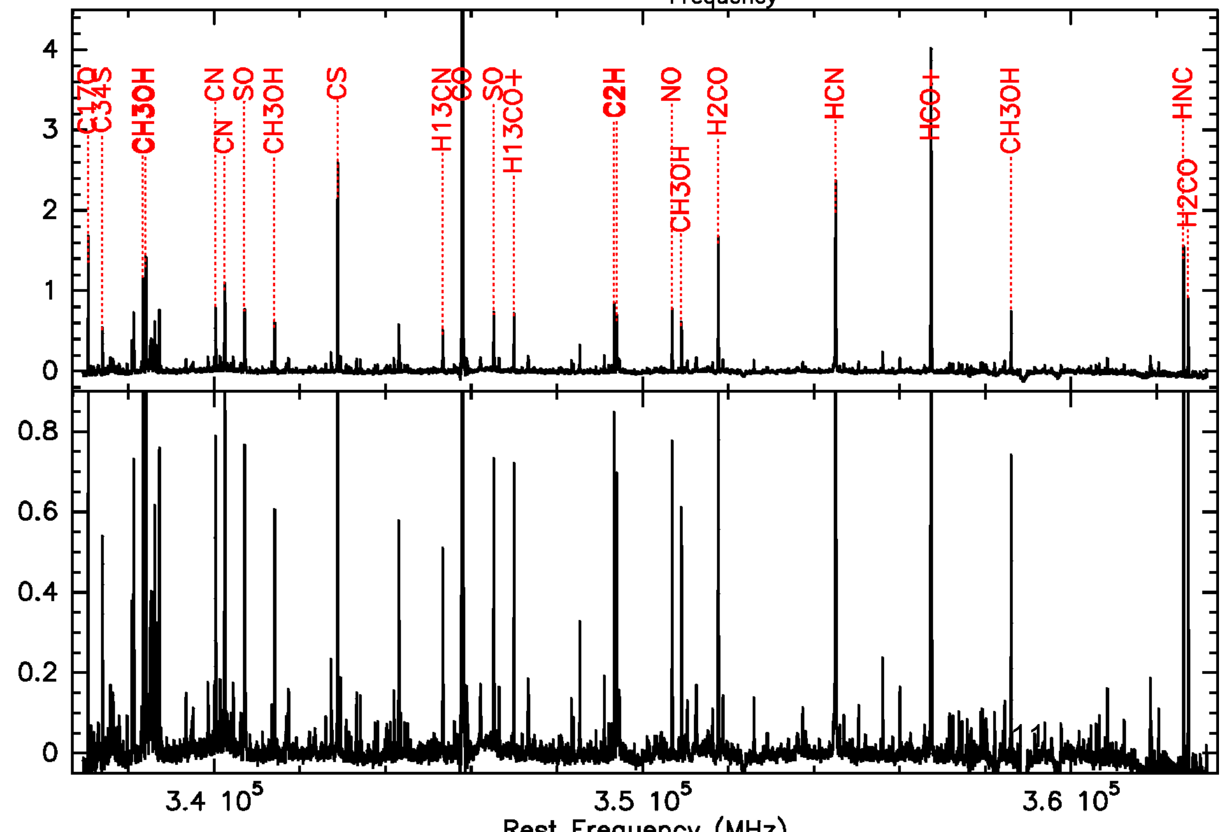

High mass star formation:

The quest for an evolutionary scheme

- Pre-protocluster cores: cold (<20K), massive (~100-1000 M)
- Pre-hot cores: IRAS sources, with/without strong MIR. "Warm" sources, T~50K
- Hot cores: internally heated, T>100K, dense (~10^7), HII region quenched
- Hyper-/ultra-compact HII regions: d<0.05pc, EM~10^9 / d<0.1pc, EM~10^7
- (compact) HII regions
- Endproducts: OB clusters/associations
- → In which stages is infall observable ?

Evidence for infall (I)

Observe infall asymmetry of optically thick spectral lines in emission:

- HMPOs, Fuller+ 2005: 0.2-1 10^{-3} $M_{\odot}$/yr
- UCHIIs, Wyrowski+ 2006, Klaassen+2008
- H_2O maser dense clumps, Wu+ 2003: B/R statistics similar to low mass clumps
- Possible earlier stages:
  - G25.38, Wu+ 2005: 3.4 10^{-3} $M_{\odot}$/yr
  - ISOSS J18339, Birkmann+ 2006
- Some cases with large scale infall → infall strong enough to overcome radiation pressure?

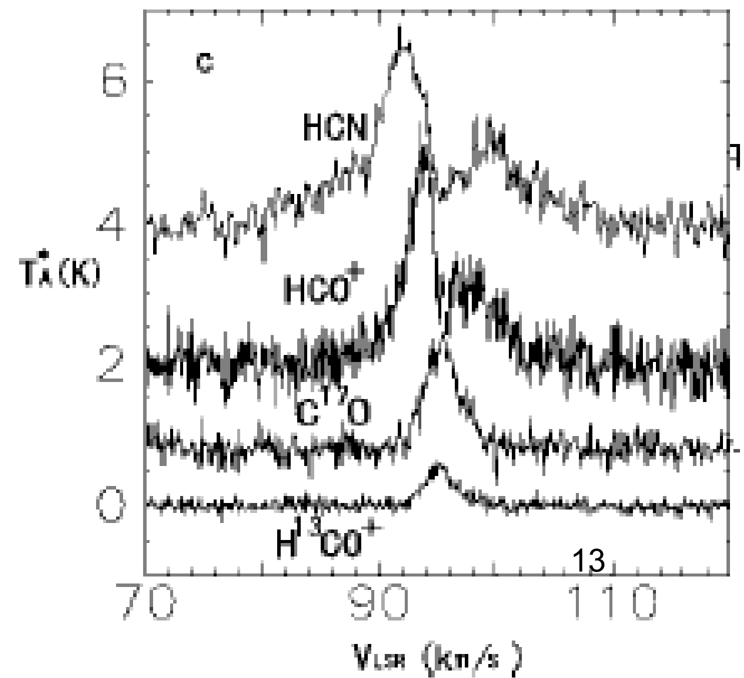

Blue skewed double peak profiles

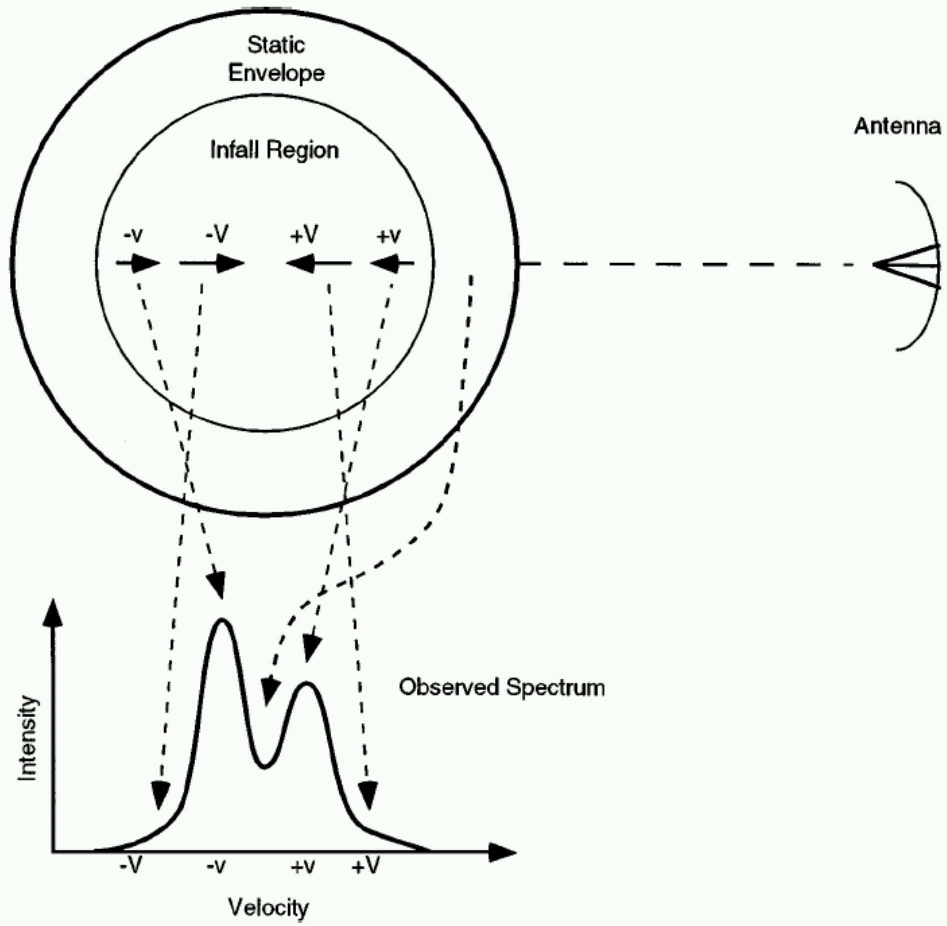

Figure 5 The origin of various parts of the line profile for a cloud undergoing inside-out collapse. The static envelope outside r_{inf} produces the central self-absorption dip, the blue peak comes from the back of the cloud, and the red peak from the front of the cloud. The faster collapse near the center produces line wings, but these are usually confused by outflow wings.

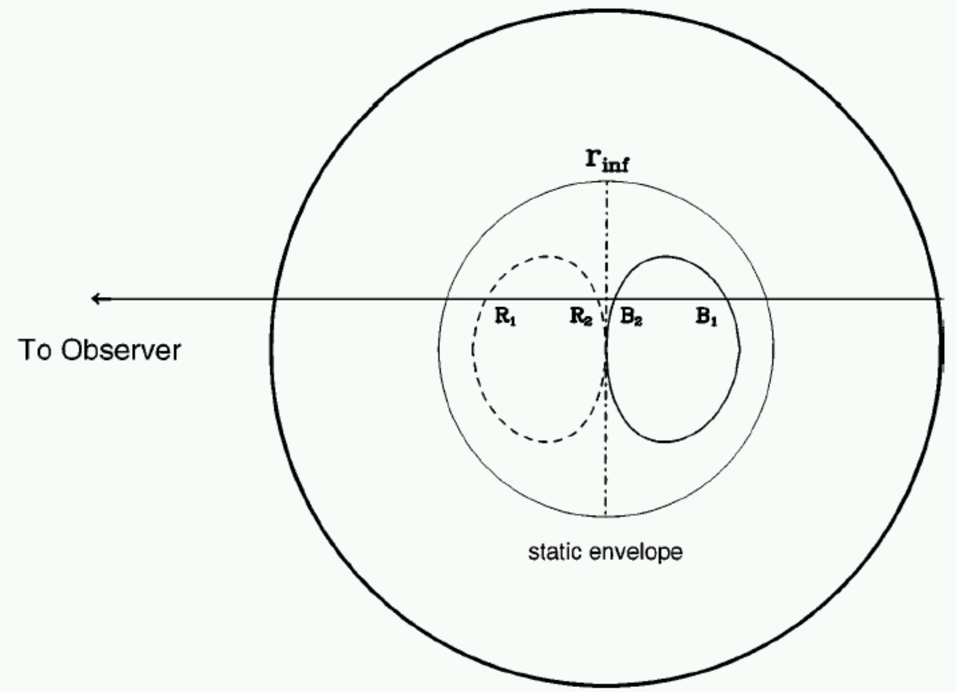

Figure 6 A schematic explanation of why line profiles of optically thick, high-excitation lines are skewed to the blue in a collapsing cloud. The *ovals* are loci of constant line-of-sight velocity, for $v(r) \propto r^{-0.5}$. Each line of sight intersects these loci at two points. The point closer to the center will have a higher T_{ex}, especially in lines that are hard to excite, so that $T_{ex}(R_2) > T_{ex}(R_1)$ and $T_{ex}(B_2) > T_{ex}(B_1)$. If the line is sufficiently opaque, the point R_1 will obscure the brighter R_2, but B_2 lies in front of B_1. The result is a profile with the blue peak stronger than the red peak (Zhou & Evans 1994).

From Evans (1999)

Predicted line profiles

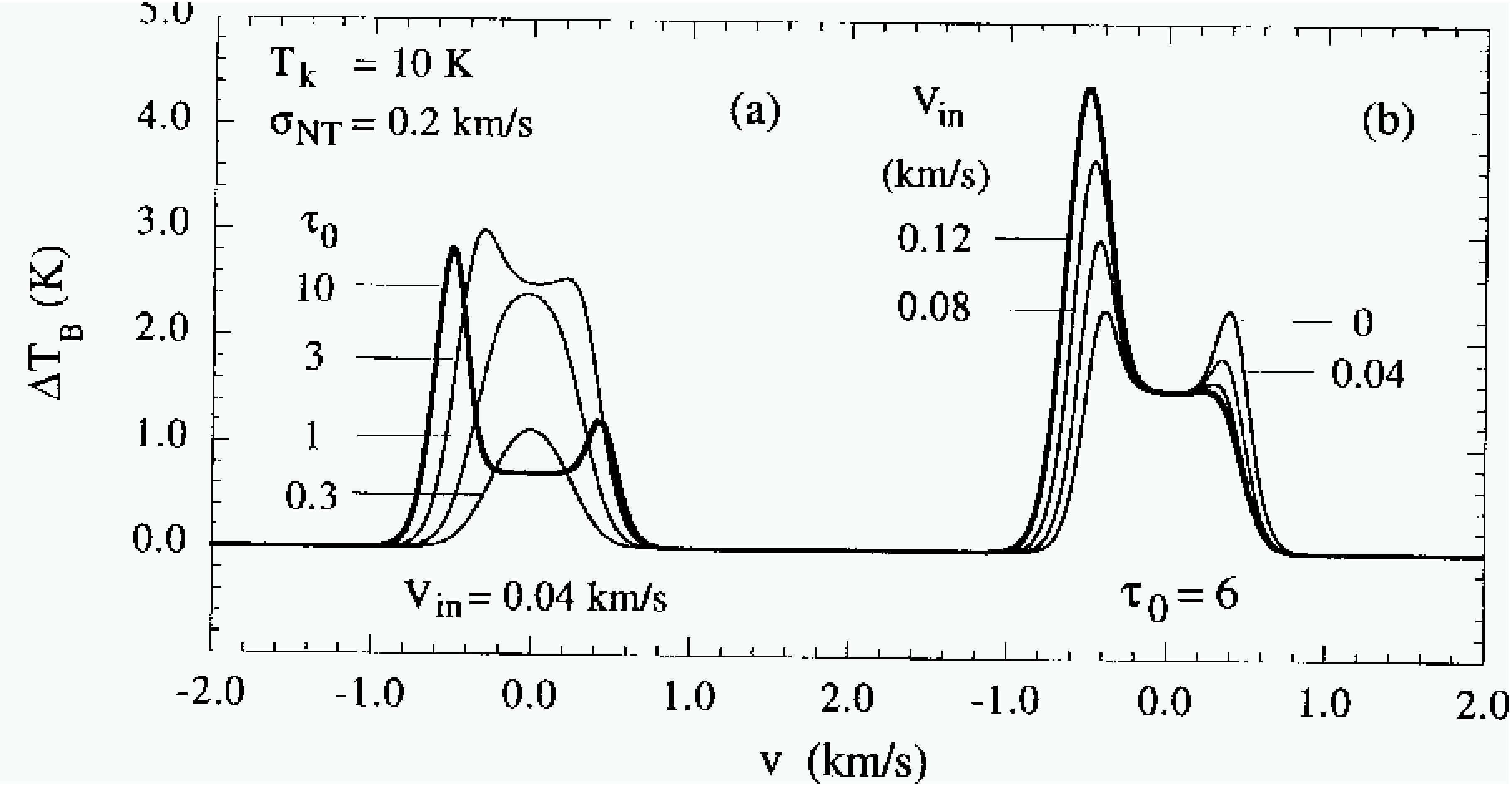

Infall rate from spectra

Myers+1996

$$v_{\rm in} = \frac{\Delta v_{\rm thin}^2}{v_{\rm red} - v_{\rm blue}} \ln\left(\frac{1 + e^{T_{\rm blue}/T_{\rm dip}}}{1 + e^{T_{\rm red}/T_{\rm dip}}}\right)$$

$$\dot{M}_{\rm in} = 4\pi R^2 n_{\rm H_2} \mu m_{\rm H} v_{\rm in} \qquad t_{\rm ff} = \sqrt{\frac{3\pi}{32 G\rho}} = \frac{3.66\times10^7\,{\rm yr}}{\sqrt{n({\rm cm}^{-3})}}$$

Table 3.4: Infall velocities, mass infall rates, and time scales for the blue excess sources

Source		$v_{\rm in}$ (km s^{-1})	$\dot{M}_{\rm in}$ (10^{-3}M$_\odot$ yr^{-1})	$\tau_{\rm in}$ (10^5 yr)	$\tau_{\rm ff}$ (10^5 yr)
Diffuse clouds					
G013.28–00.34...	MM1	0.45(0.15)	0.6	1.6	1.5
G013.97–00.44...	MM1	0.32(0.13)	-	-	-
Peaked clouds					
G013.91–00.51...	MM1	2.71(0.10)	8.6	0.17	0.70
G024.94–00.15...	MM1	1.38(0.12)	3.4	0.31	0.74
	MM2	1.08(0.13)	2.2	0.39	0.78
G030.90+00.00...	MM2	1.57(0.15)	90.2	0.08	1.5
G035.49–00.30...	MM1	1.81(0.13)	4.1	0.24	0.78
	MM2	0.50(0.10)	8.6	0.08	0.85
G053.81–00.00...	MM1	4.82(0.10)	6.3	0.04	0.55
Multiply peaked clouds					
G017.19+00.81...	MM2	2.08(0.20)	9.7	0.15	0.42
	MM3	6.65(0.13)	11.5	0.06	0.85
G018.26–00.24...	MM3	5.46(0.18)	14.4	0.09	0.80

Rygl+2012

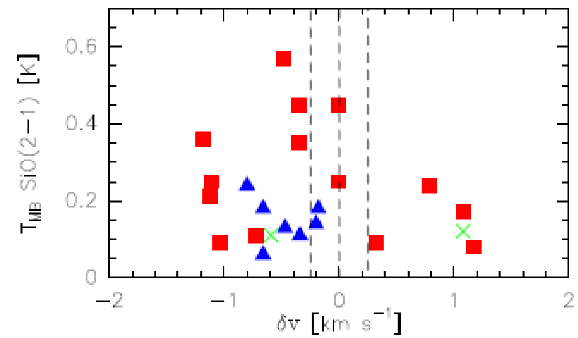

Fig. 9. SiO detections against the skewness parameter δv. The skewness parameter which is significant if $|\delta v| > 0.25$, marked by the outer dashed lines. A negative δv indicates infall, while a positive δv outflow or expansion. The green crosses represent sources in diffuse clouds, the blue triangles clumps in peaked clouds, and the red squares represent sources in multiply peaked clouds.

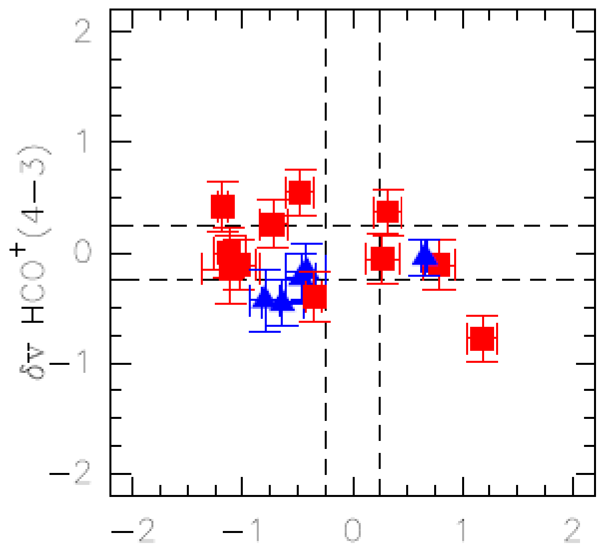
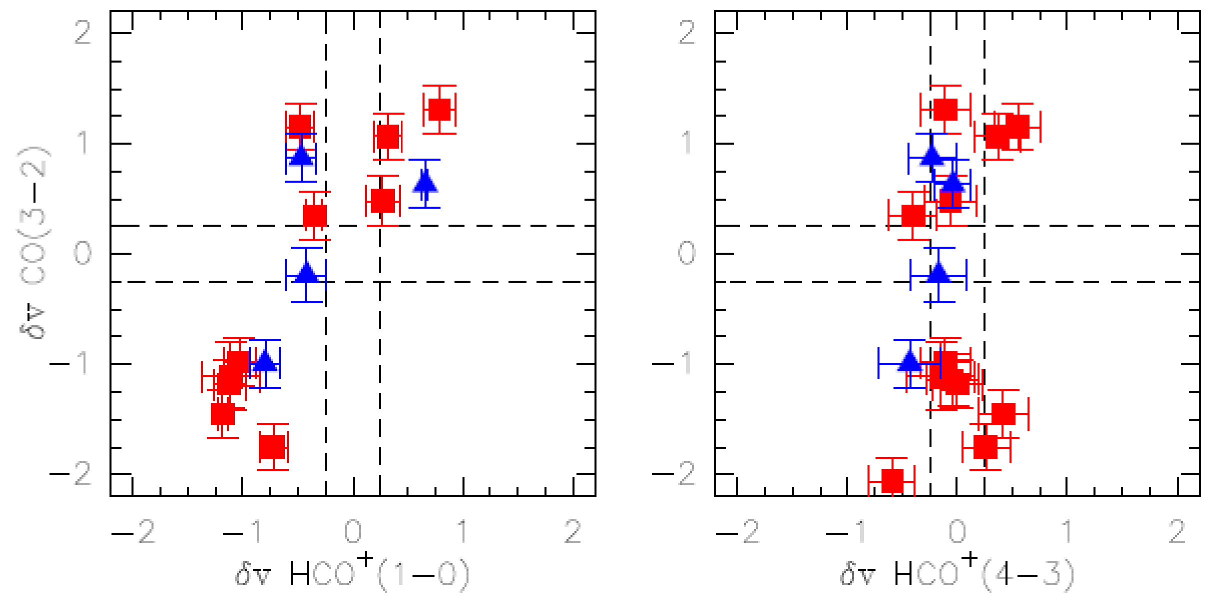

Fig. 3. The skewness parameter of the HCO$^+$(1–0) line versus that of the HCO$^+$(4–3) and ^{12}CO(3–2) lines. The dashed lines mark the boundary of significant excess at $\delta v > |0.25|$. The blue triangles represent clumps in peaked clouds, while the red squares represent sources in multiply peaked clouds.

Evans (1999): "path towards salvation"

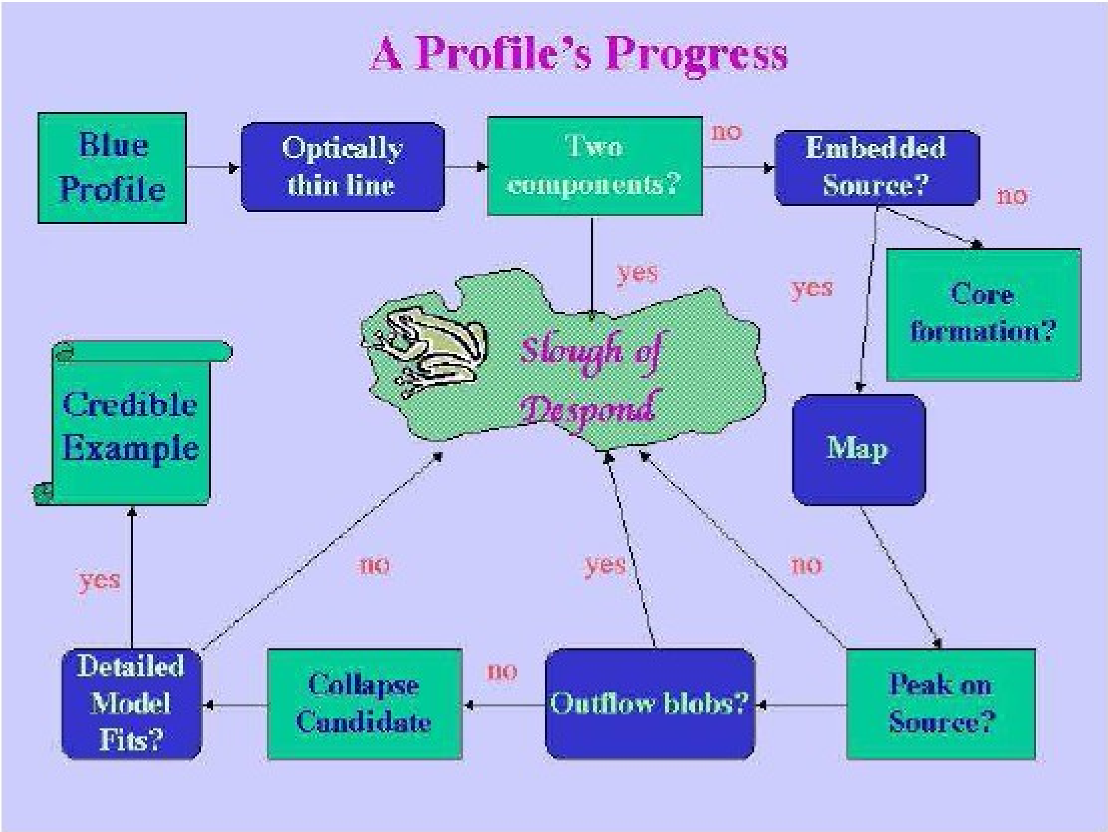

Figure 4. The progress of a blue profile through the many pitfalls on the path toward "salvation," as a credible example of collapse (with apologies to John Bunyan).

And issue of changing abundances not even mentioned ...

Inverse P Cygni profiles

Klassen+2011 (SMA)

P. D. Klaassen et al.: High Resolution CO Observation of Massive Star Forming Regions

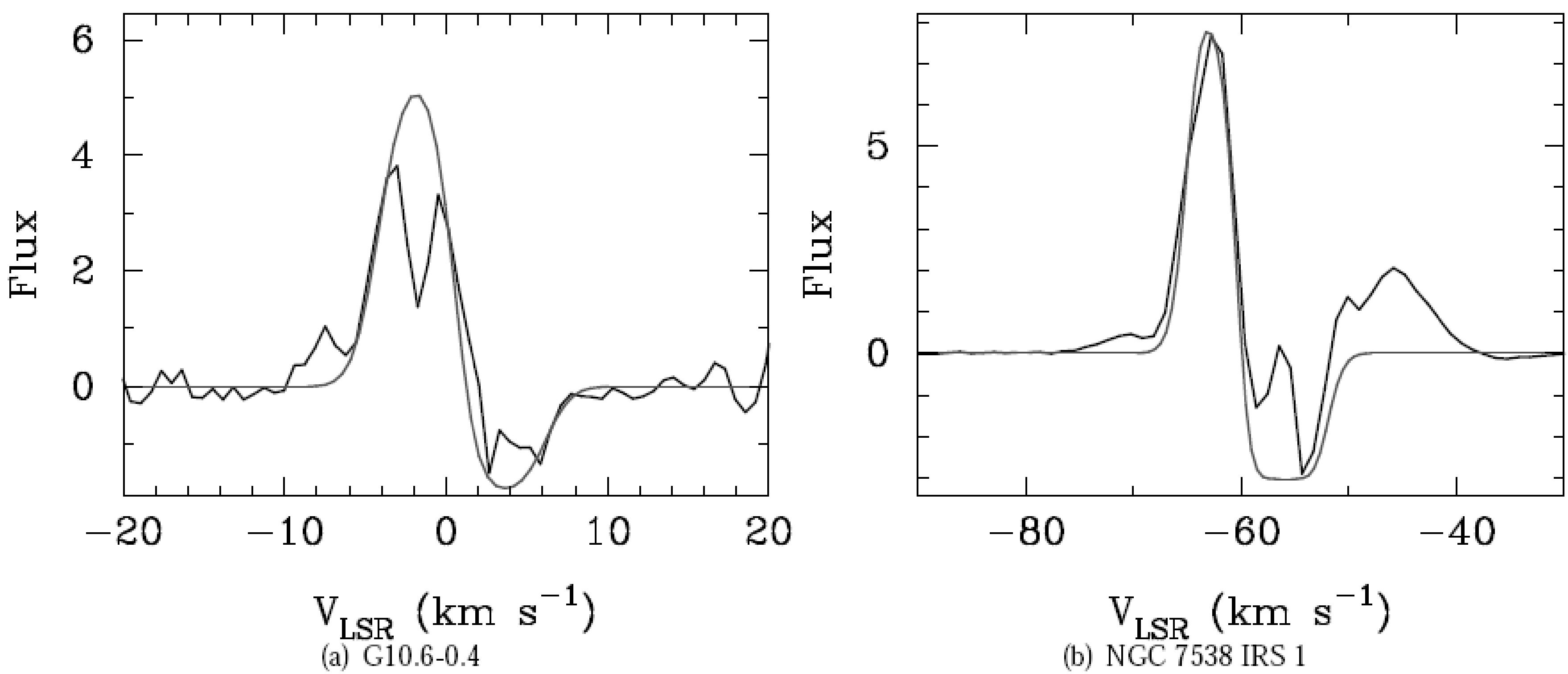

Fig. 2. CO (J=2-1) spectra integrated over the infall regions overlapping with the HII regions for G10.6 (left) and NGC 7538 (right). The grey lines shows the 2 layer infall model characterized by the parameters given in Table 4.

infall rates of order 10^{-4} $\dot{M}_\odot$ yr^{-1}

Evidence for infall (II)

Observe infall as redshifted absorption in front of strong cm continuum from UCHIIRs:

- Zhang+Ho1997: W51
- Keto++, Sollins+2005: G10.62
- Beltran+2006: G24.78
- Beuther+2009:
  ATCA southern sources
- → Accretion of up to 10^{-3} $M_\odot$/yr
- Accretion even through UCHII?
- Only late stage probed :-(

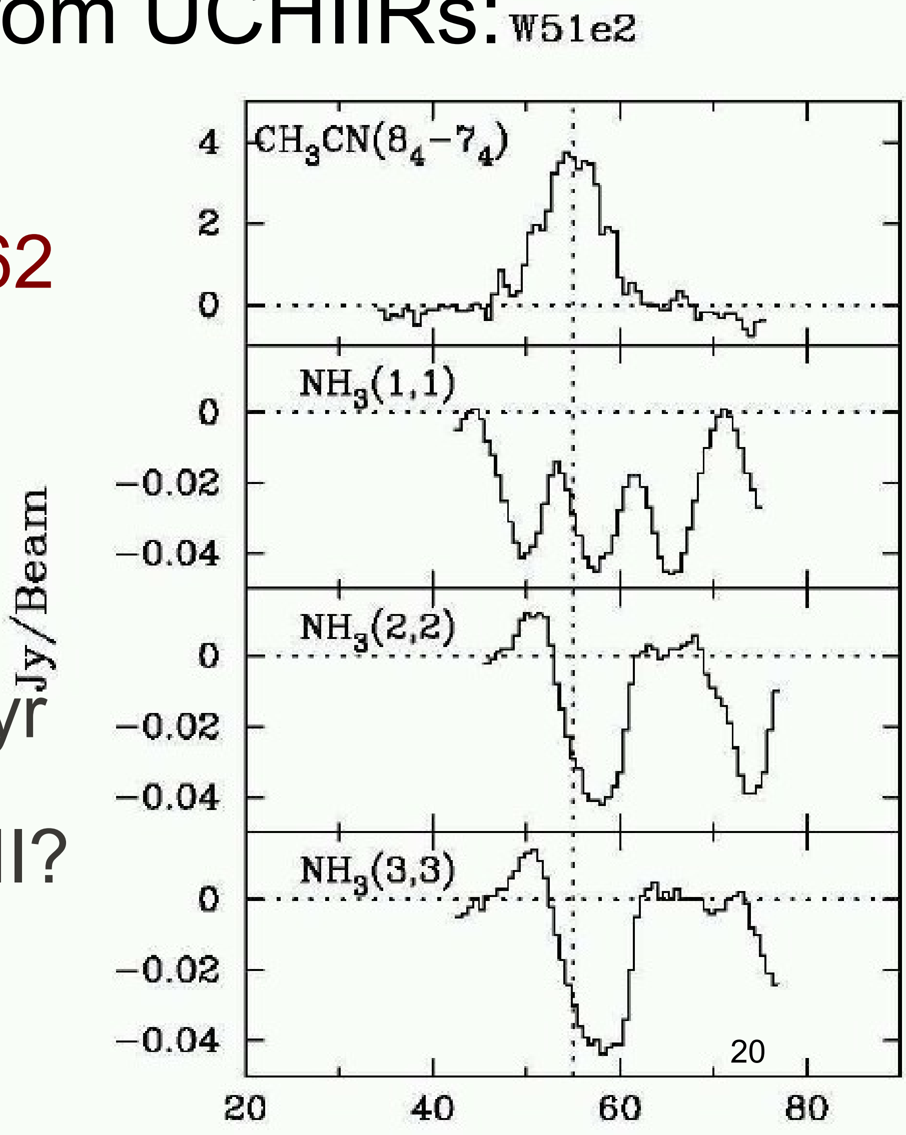

Infall towards G24

Beltran+2006

- Cm cont: O9.5 star
- $\dot{M}_{\rm acc} \approx \Omega/(4\pi)[4\times10^{-4}–10^{-2}]M_\odot\,{\rm yr}^{-1}$.
- Would quench HII region
- → non-spherical accretion
- See also Sollins/Keto papers on accretion through HII regions

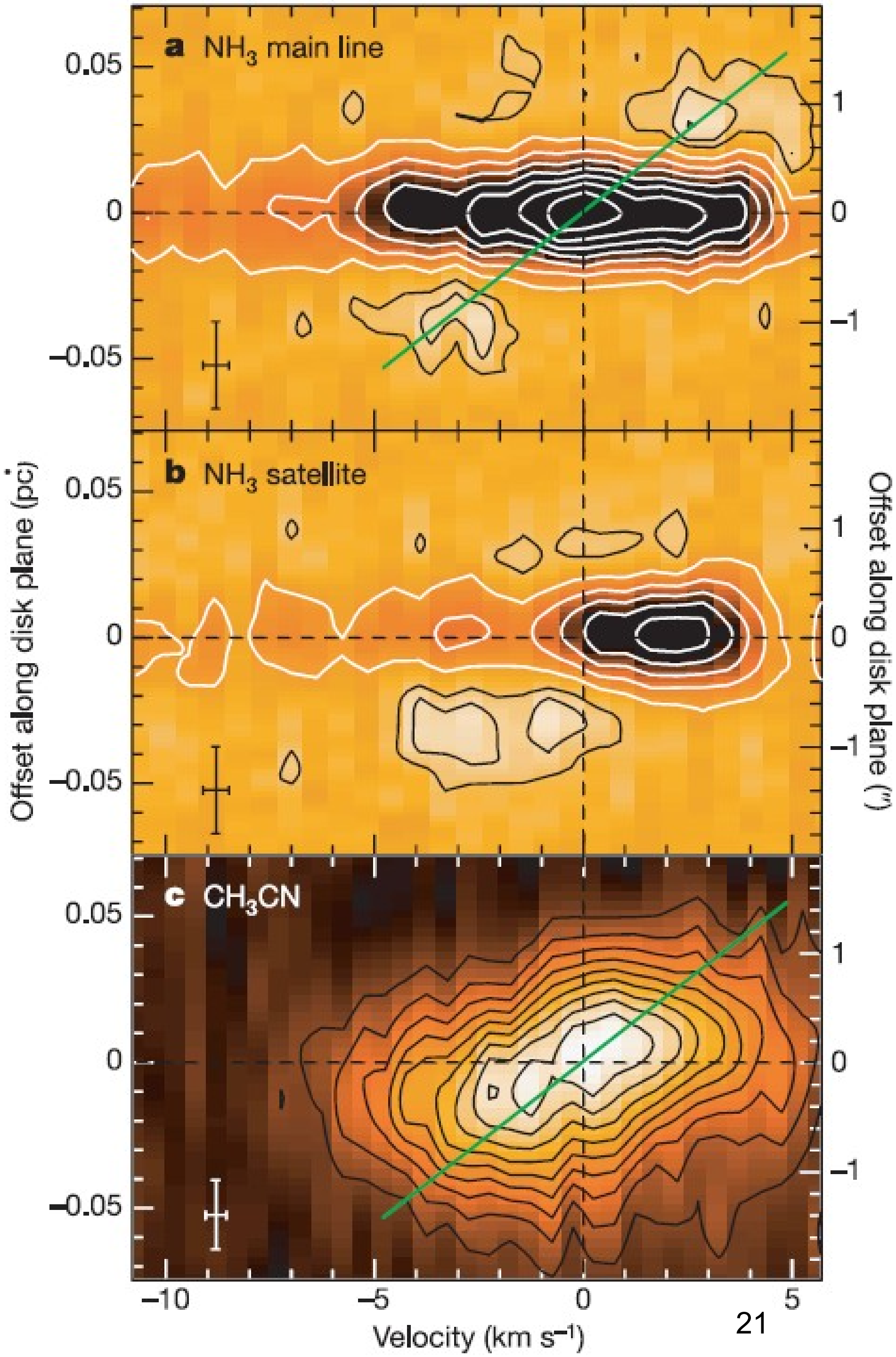

Figure 2 | Velocity field in the massive toroid G24 A1. a, Position–veloci

Ammonia

- cm: Inversion lines
- FIR: Rotational lines
- overabundant in hot cores, apparently no depletion in cold sources

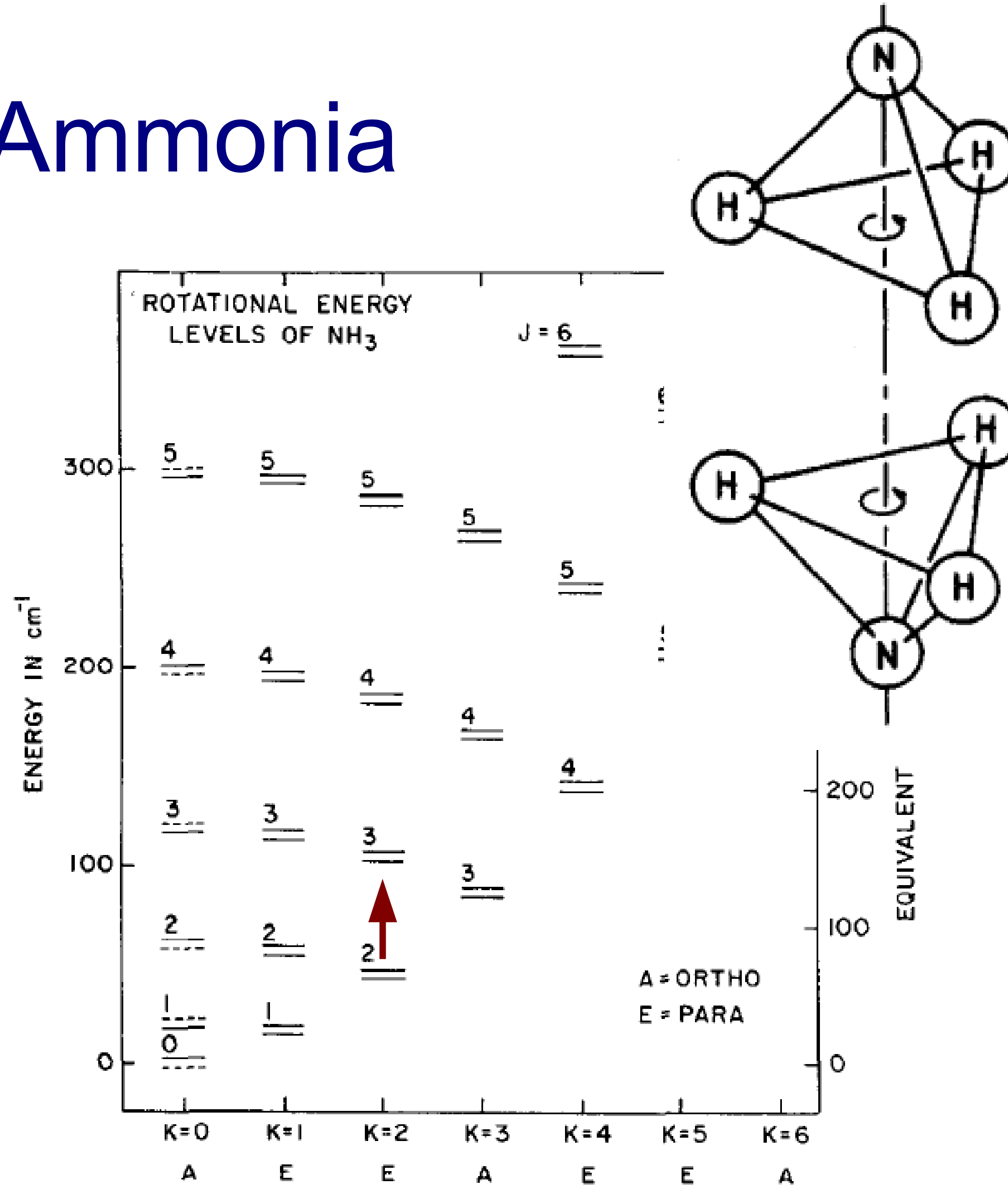

Figure 1 Energy level diagram of rotation-inversion states. *J* is the total angular-momentum quantum number, and *K* is the projected angular momentum along the molecular axis.

Science objectives

- Ammonia as a probe of infall in HMSF regions
  - Study rotational transition
  - Determine infall rates on LOS (pencil beam)
  - Explore absorption of THz lines in front of dust continuum as new tool
  - Probe ammonia abundance in envelope
  - Study infall through the evolution of massive clumps using ATLASGAL as target finder

Sample taken from ATLASGAL (& WISH)

3 sources observed

Table 1: Ammonia source sample.

Source	Ra (J2000) (h m s)	Dec (° ′ ″)	V_{lsr} (km s^{-1})	L_{bol} ($L_{\odot}$)	d (kpc)	S(870μm) (mJy/bm)
IRDC						
AG23.20–0.38	18 34 54.9	−08 49 19	+77.9	–	4.6	6.4
mIR-quiet HMPO						
W43-MM1	18 47 47.0	−01 54 28	+98.8	2.3×10^4	5.5	21.2
mIR-bright HMPO						
IRAS18089−1732	18 11 51.5	−17 31 29	+33.8	3.2×10^4	3.6	8.5
Hot Molecular Core						
G31.41+0.31	18 47 34.3	−01 12 46	+98.8	1.8×10^5	7.9	21.2
UC HII Region						
G34.26+0.15	18 53 18.6	+01 14 58	+57.2	2.8×10^5	3.3	44.7

G34.26

- Stage: UCHII w. associated HC
- Proto-typical cometary HII r.
- 3.7 kpc
- L=3E5
- Ext. vs int. heating debate

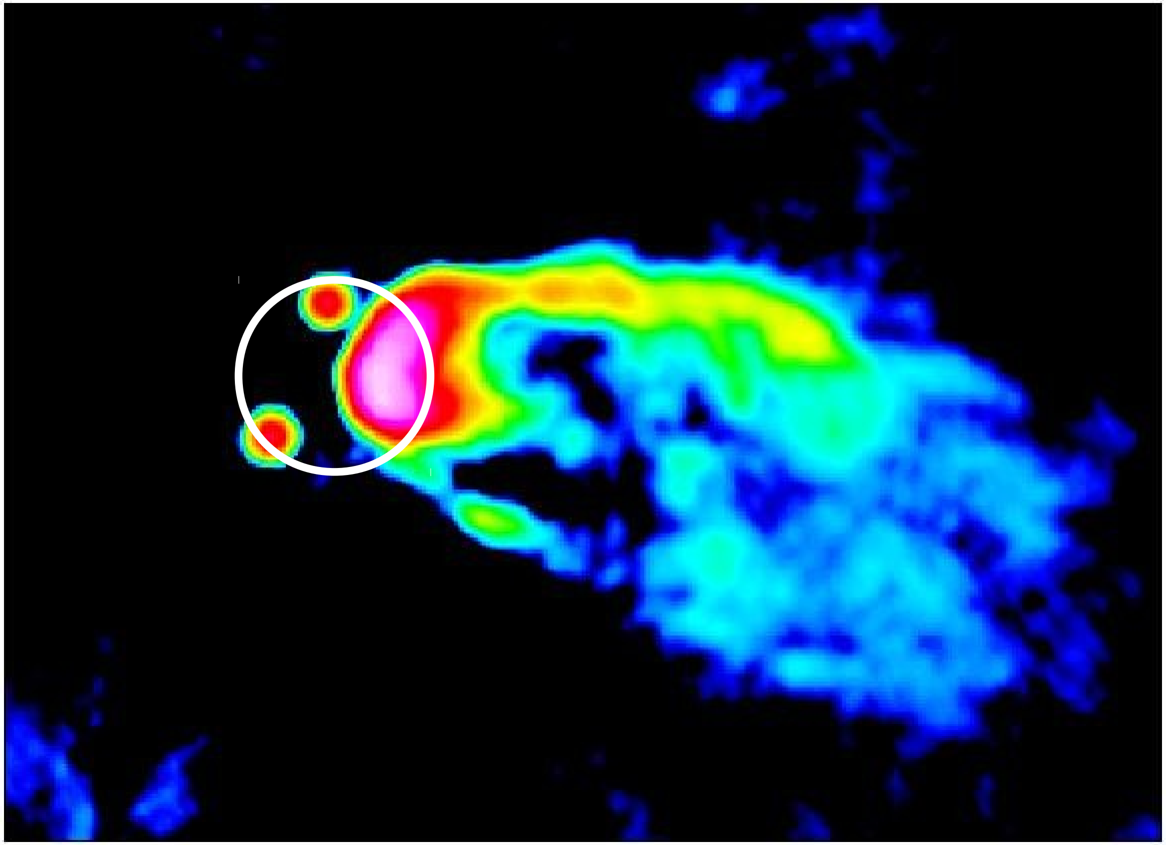

G34.26+0.15 VLA X band

Watt&Mundy 1999 (CH_3CN)

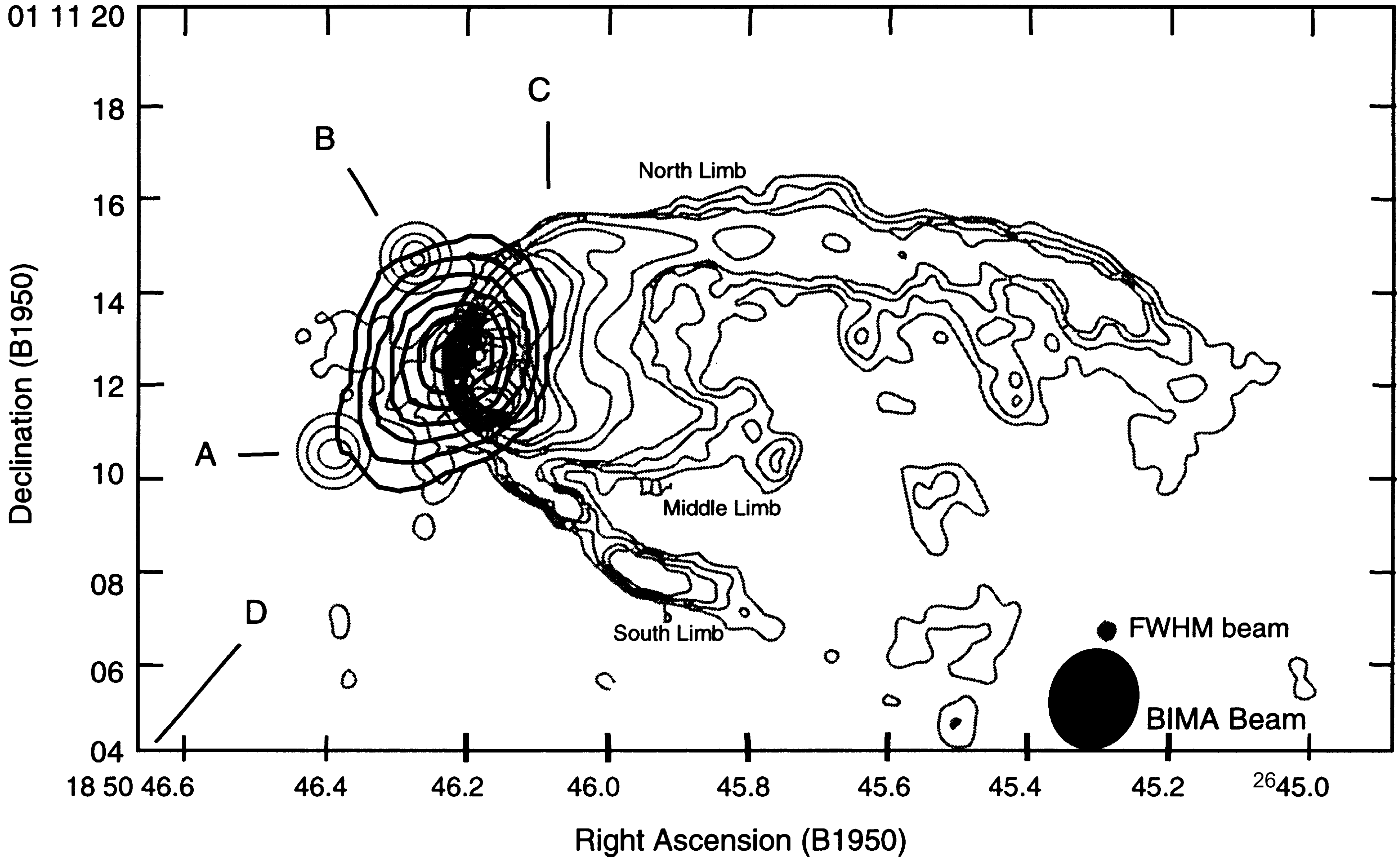

G31.41+0.31

- Stage: Hot core offset from HII region
- Proto-typical cometary HII r.
- 7.9 kpc
- L=2E5
- Massive toroid

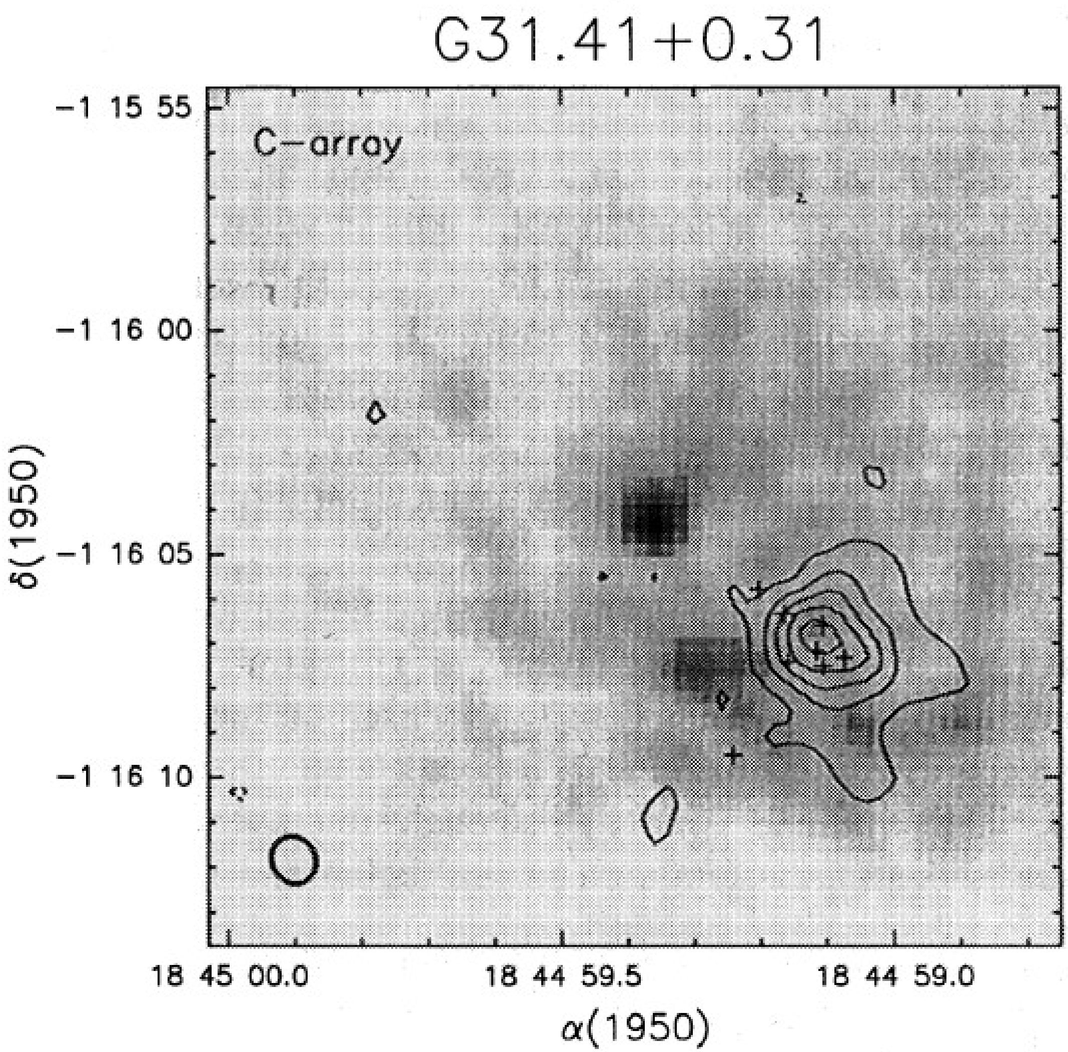

VLA K band, NH3 (4,4)
Cesaroni+1994

W43-MM1

- Coldest and most massive core in W43 mini-starburst region (Motte+2003)
- 5.5 kpc
- L=2E4
- cm/MIR quiet

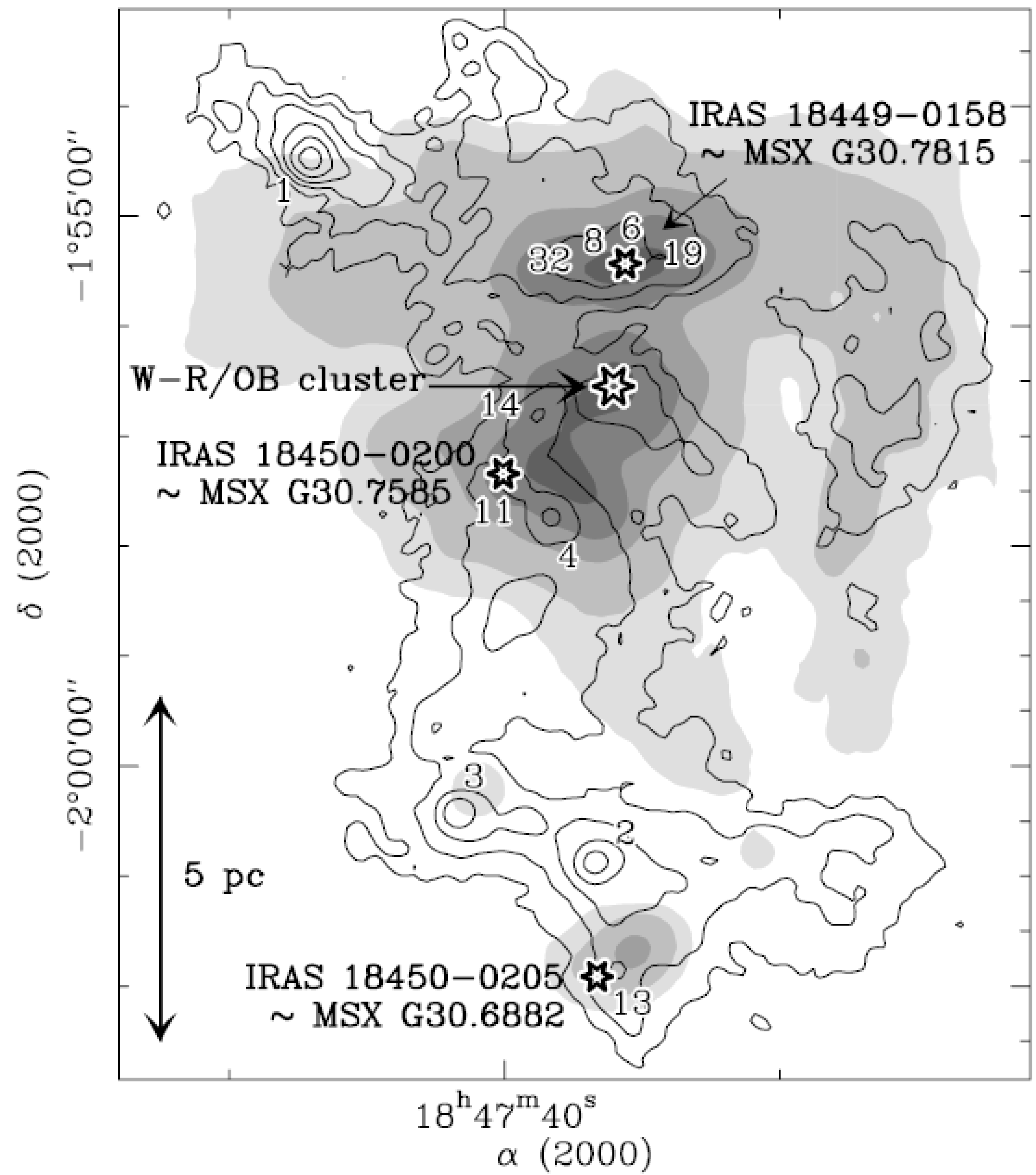

FIG. 6.—Continuum emission of W43 at 21 μm (*gray scale*) compared with that at 1.3 mm (*contours*). The 21 μm map was obtained by the *MSX* satellite with a 20″ aperture. Levels are 0.5, 1, 3, 6, and 12 × 10^9 Jy sr^{-1}. The 1.3 mm map is shown in Fig. 1*a* with the same contours, except the first one. *IRAS*/*MSX* sources and the W-R/OB association are indicated by star symbols; selected submillimeter fragments are labeled.

Herschel water results

M.G. Marseille et al.: Water abundance measurements in high-mass protostars: Herschel observations with HIFI

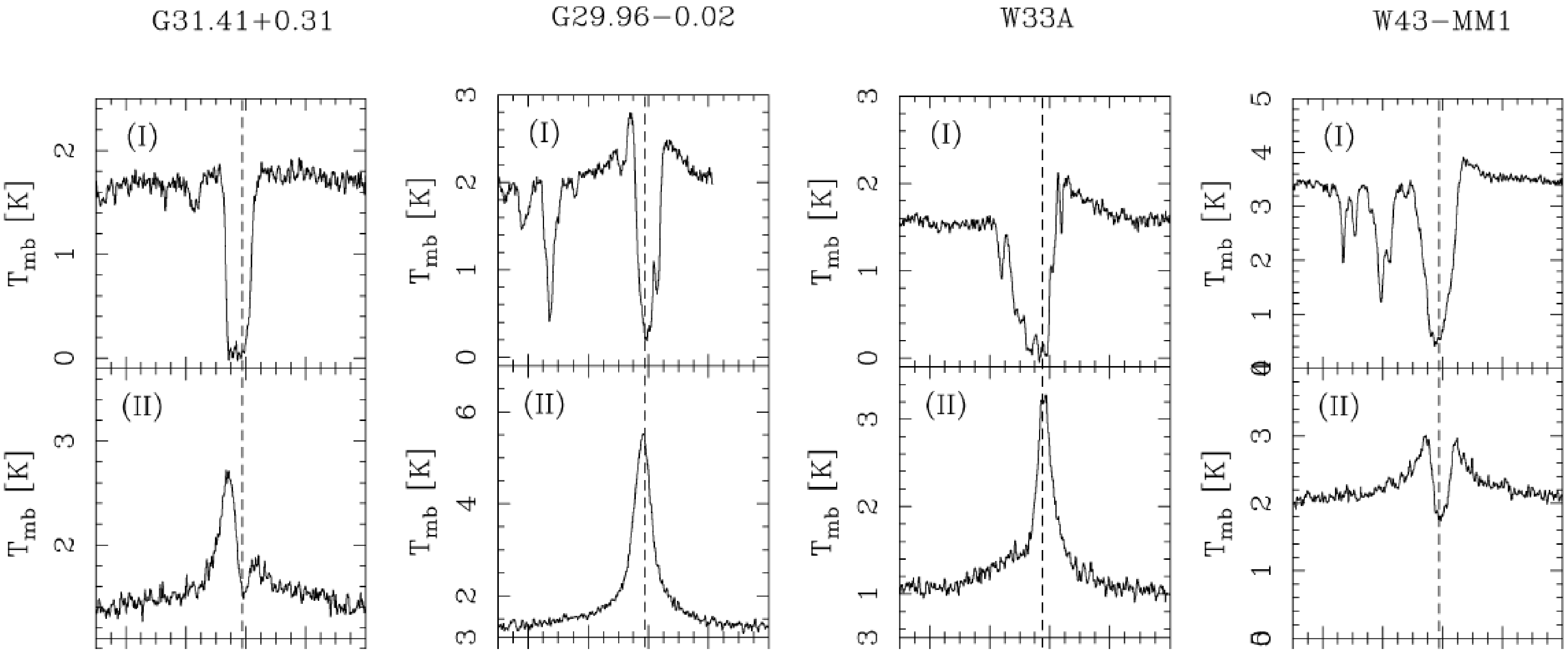

Hily-Blant+2010
IRAS16293
HIFI

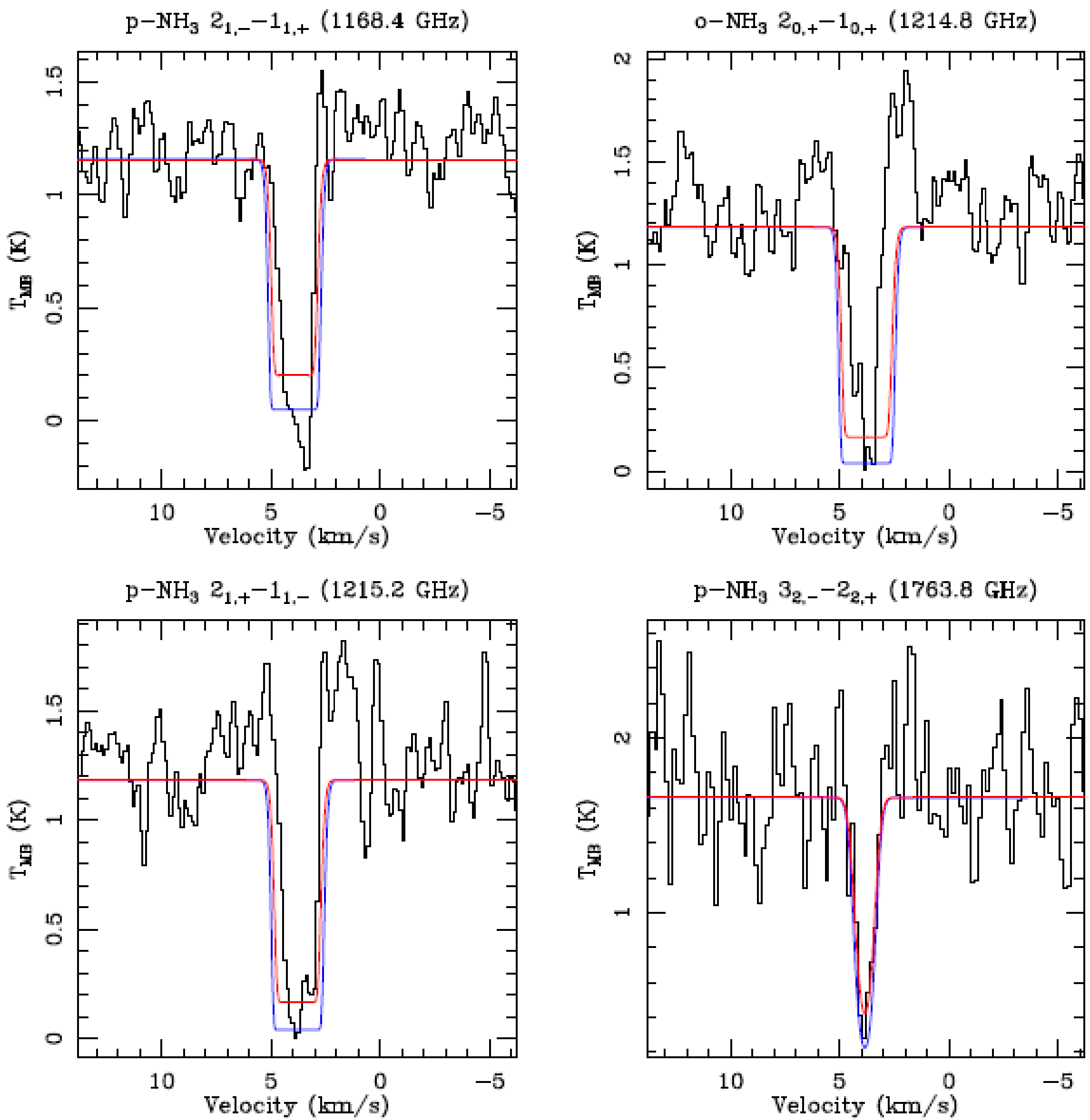

Fig. 2. NH_3 absorption lines from 1.168 to 1.764 THz. LTE predictions are shown in red (T_{ex}=10 K, $N(NH_3)$ = 3.5×10^{15} cm^{-2}) and blue (T_{ex} = 8 K, $N(NH_3)$ = 2×10^{16} cm^{-2}).

SOFIA Observations

- Basic Science flight 04 (July 20)
- GREAT:
  - CO (13-12) 1496.922 USB
  - NH_3 3_{2+}-2_{2-} 1810.379 LSB (spare 1.9THz LO)
  - 2 FFTS:1.5 GHz (8192 channels)
  - Chopped observations of 3 sources
  - About 10' each source

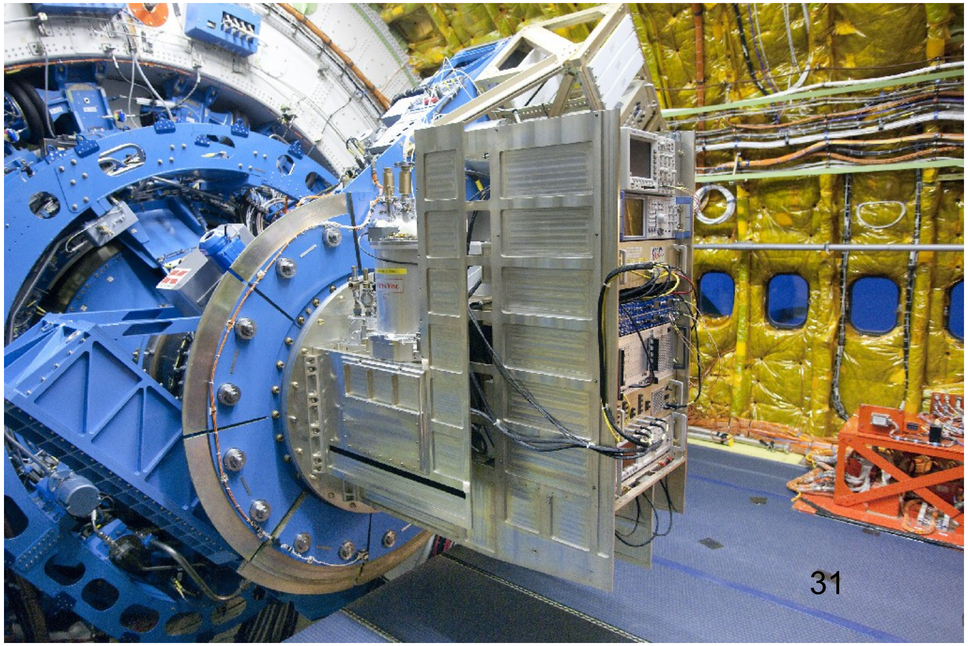

Transmission @ NH_3

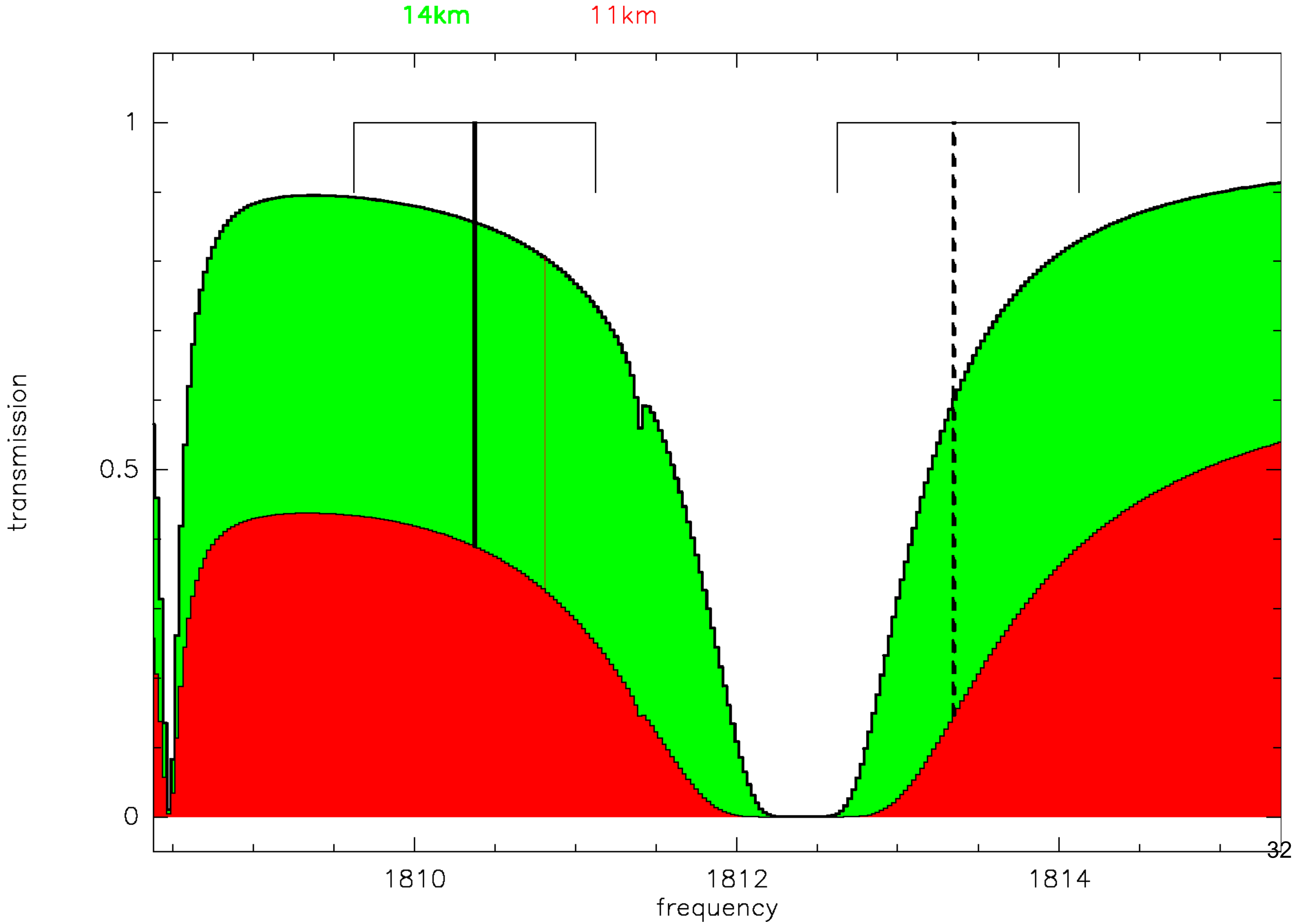

Ammonia@1.8THz

- 3 absorption line detections
- All redshifted with respect to v_sys
- $\tau \sim 1$

Table 2. Line parameters from Gaussian fits to the NH_3 lines. Nominal fit errors are given in brackets. In addition, the velocity of $C^{17}O$ (3–2) lines observed with the APEX telescope are given.

Source	T_{peak} (K)	Δv (km s^{-1})	$V_{LSR}^{NH_3}$ (km s^{-1})	$V_{LSR}^{C^{17}O}$ (km s^{-1})
W43-MM1	–0.96 (0.22)	5.3 (0.8)	99.7 (0.4)	97.65 (0.06)
G31.41+0.31	–1.18 (0.29)	3.7 (0.8)	99.4 (0.4)	97.02 (0.04)
G34.26+0.15	–3.38 (0.56)	5.5 (0.6)	61.2 (0.3)	58.12 (0.03)

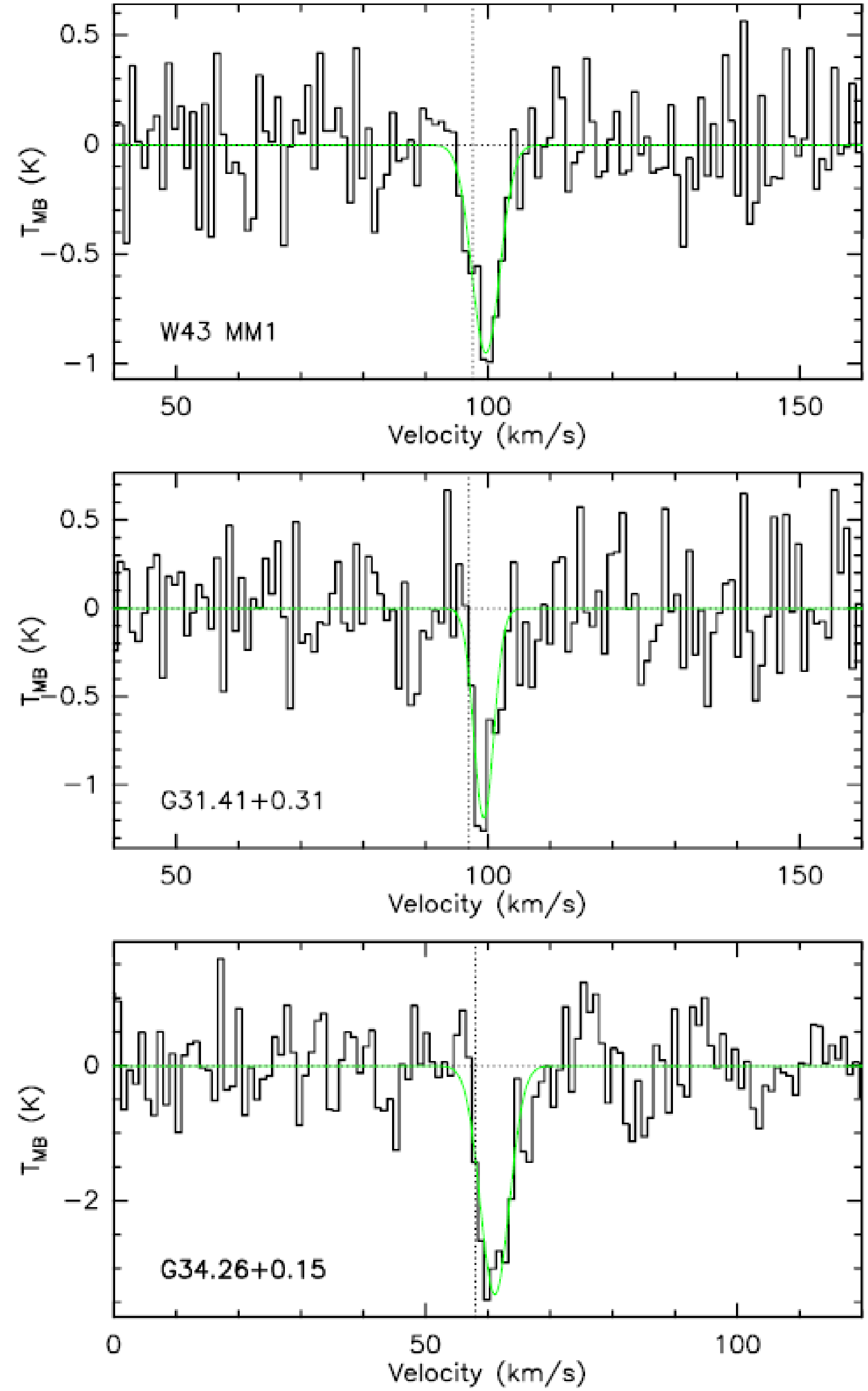

ig. 2. NH_3 spectra of the observed sources. Results of Gaussian fits o the line are overlaid in green. The systemic velocities of the sources, letermined using $C^{17}O$ (3–2) are shown with dotted lines.

G34: comparison to VLA absorption

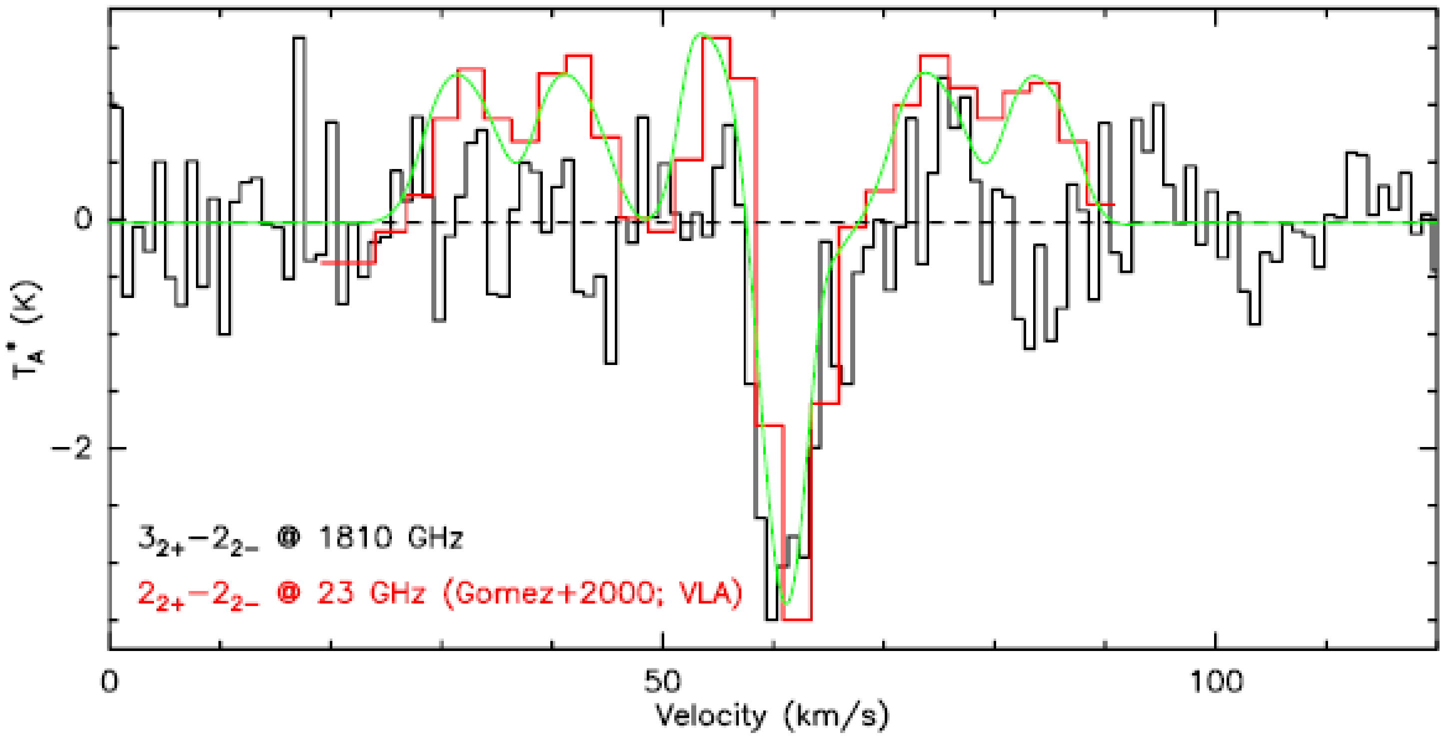

Fig. 3. G34.26+0.15 SOFIA NH_3 spectrum compared with the VLA NH_3 (2,2) spectrum taken from Gómez et al. (2000) which was integrated over the region which shows absorption. A two-component hyperfine fit to the (2,2) spectrum is shown in green.

RATRAN modelling

- Based on Rolffs+2010:
  - Fit continuum (ATLASGAL) with density power law
  - Temperature structure dictated by inner heating source
  - Velocity structure as fraction of free-fall

Rolffs+2010

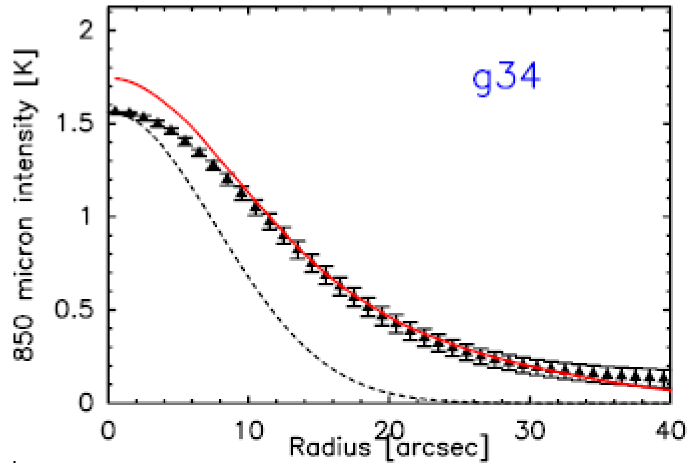

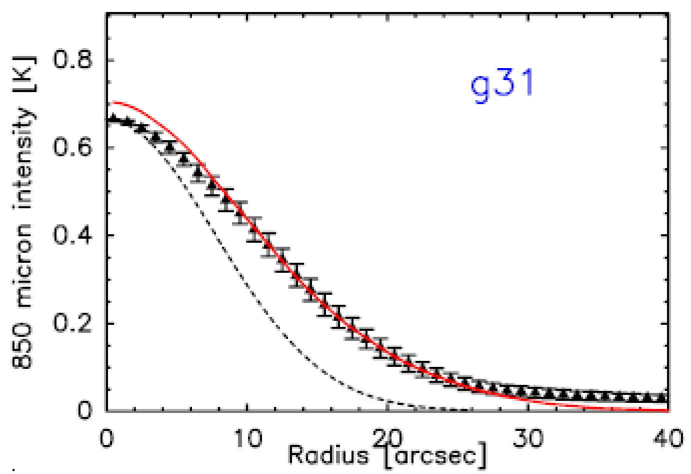

RATRAN modelling II

- Adjust to Herschel/SOFIA continuum
  - Dust properties
  - 2nd warm component

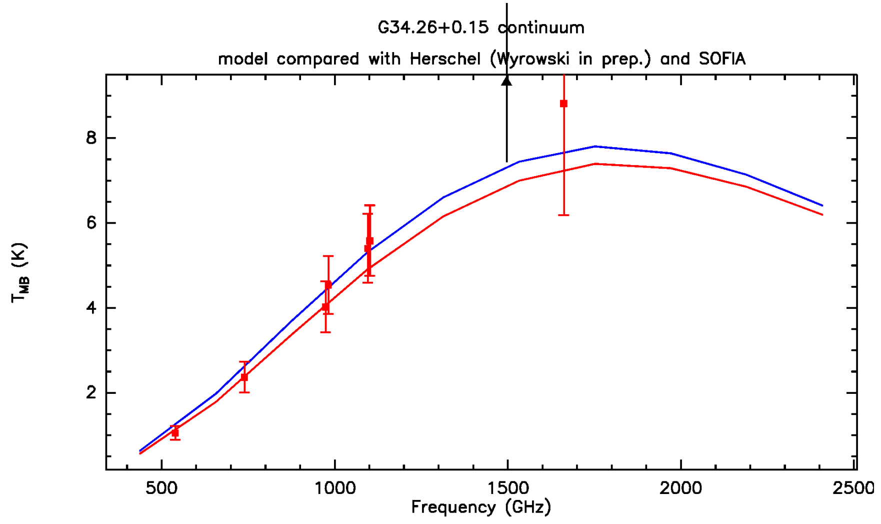

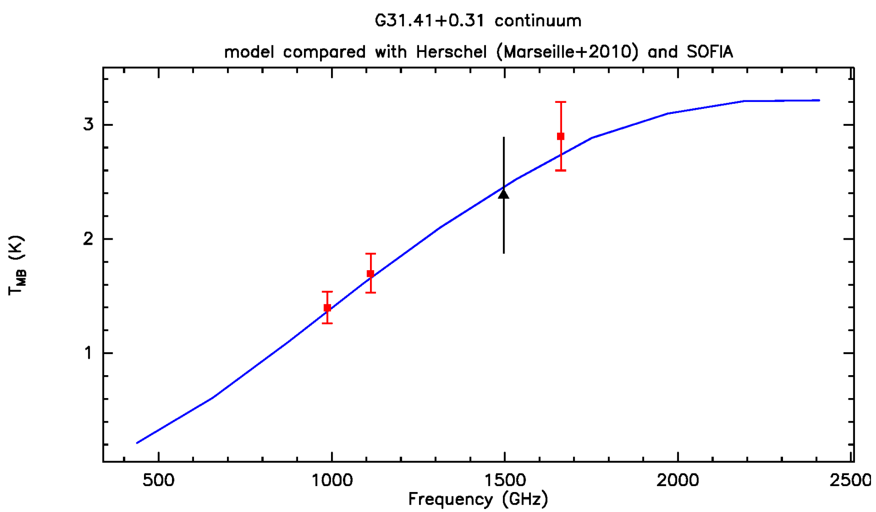

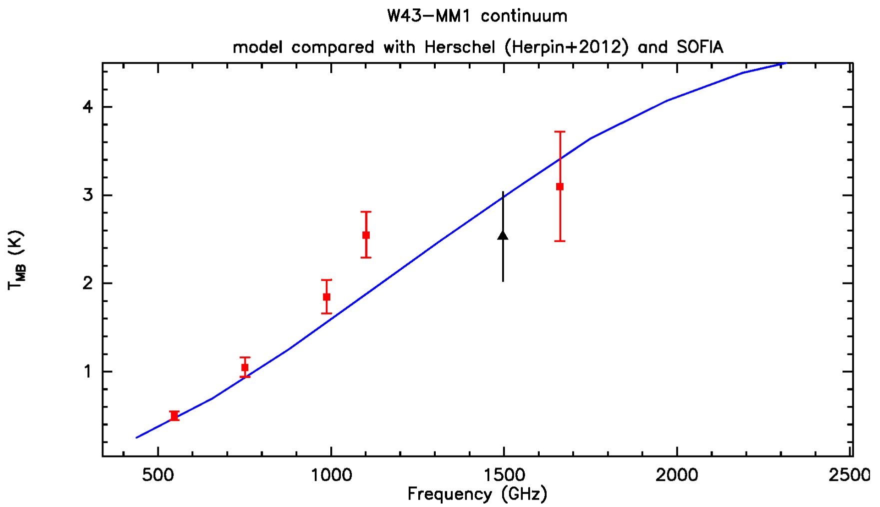

RATRAN modelling III

- Adjust NH_3 abundances and velocity field
  - Hot core + cold clump
  - Free fall fraction

G34.26

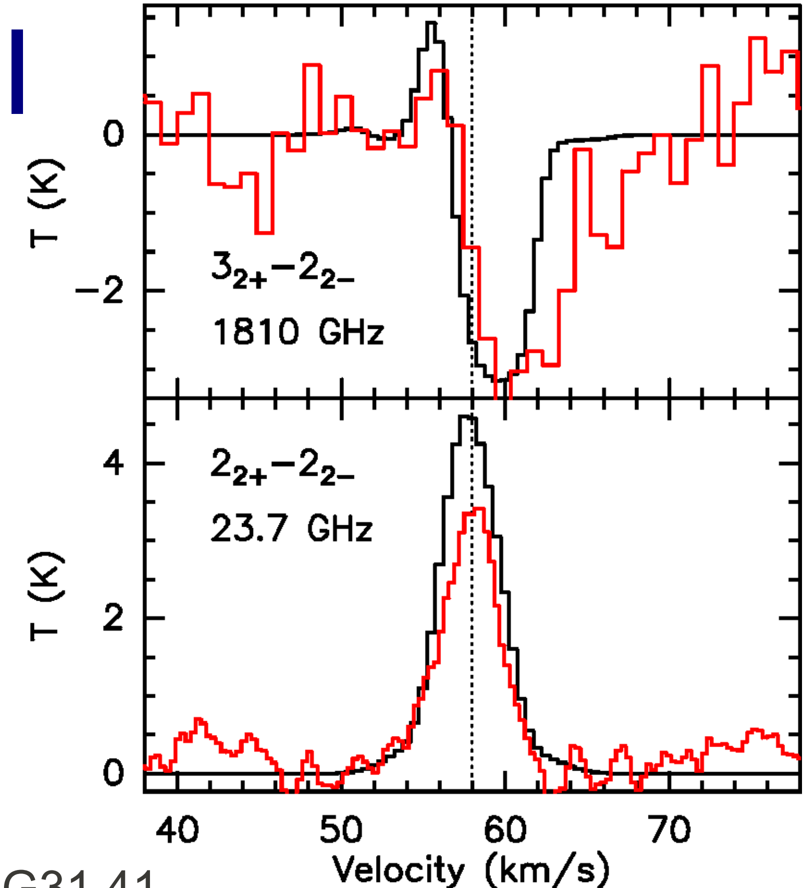

W43-MM1

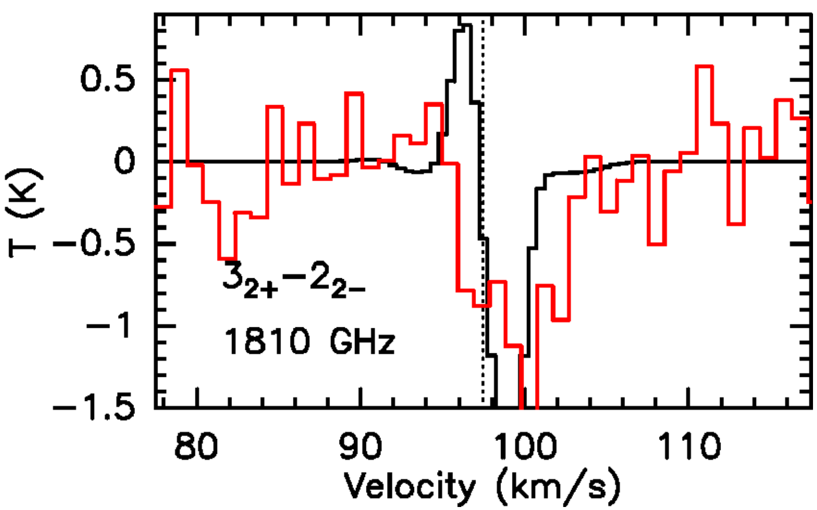

G31.41

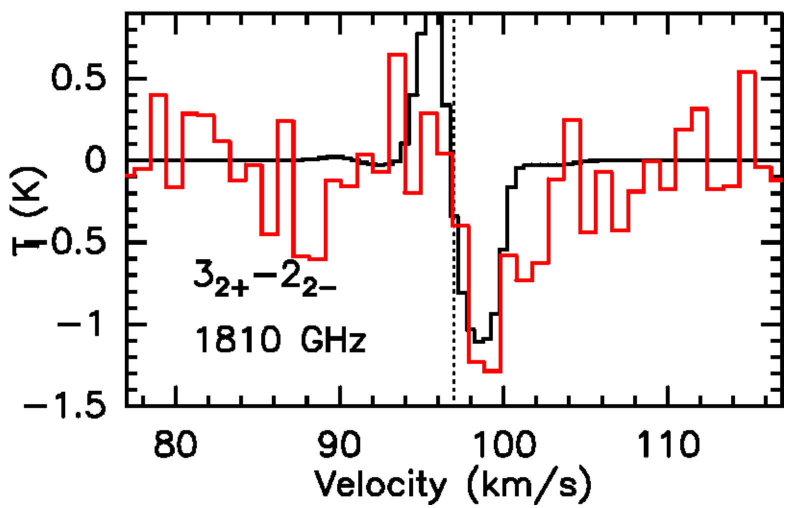

Results

- Hot core abundance poorly constrained
- In T<100K envelope ~ 2 x 10^{-8}
- 20% of free-fall needed to reproduce observed redshifted absorption
- Infall rates of 3-10 x 10^{-3} $M_{\odot}$/yr
- Evidence for further excess redshifted absorption, currently not fit, might originate from hot core

Complementary data

- Effelsberg NH3 (2,2)
- APEX emission infall profiles:
  - e.g. HNC (4-3)

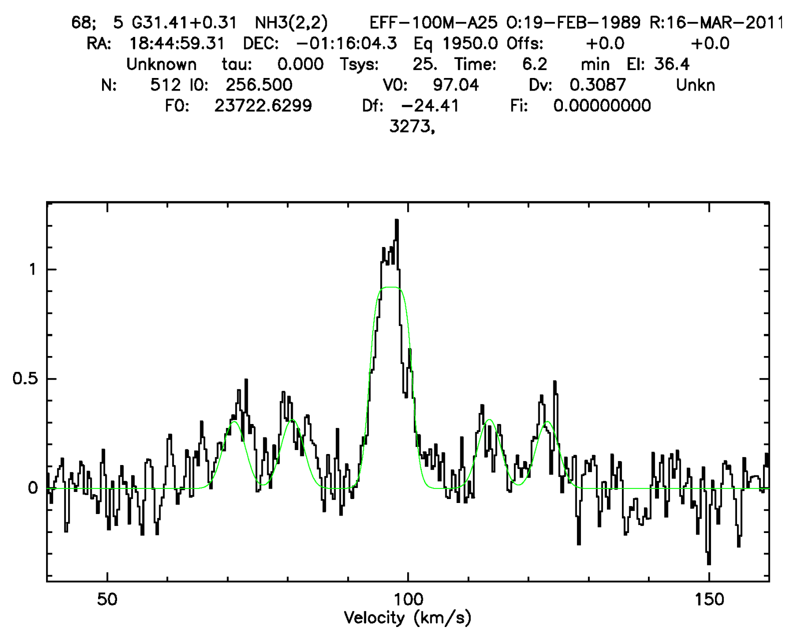

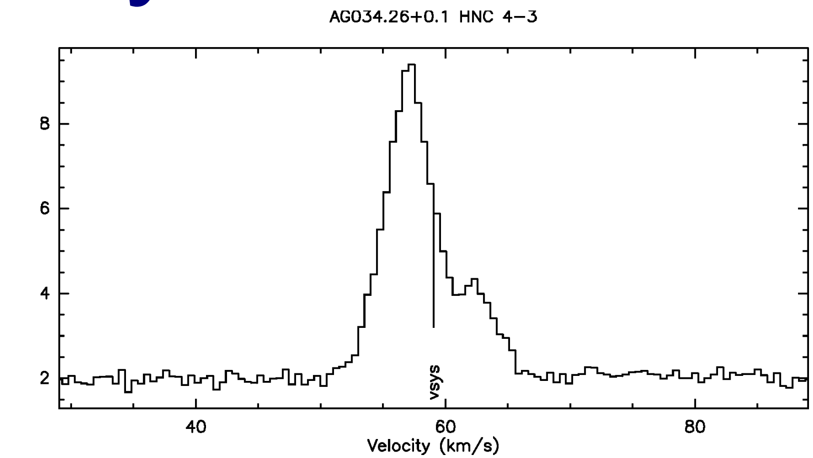

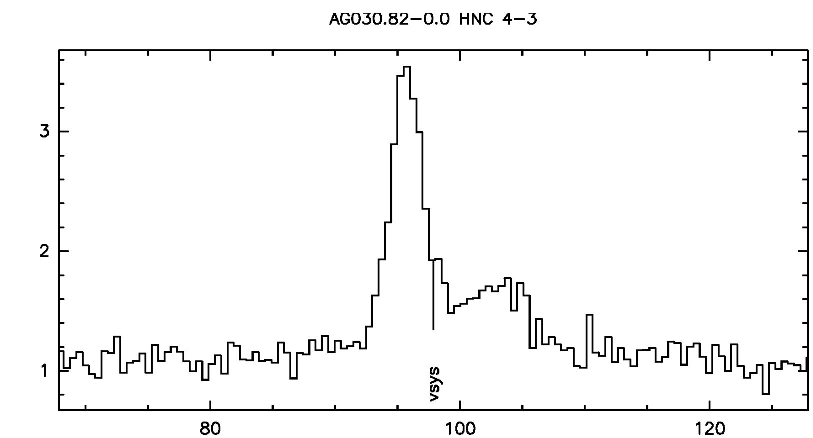

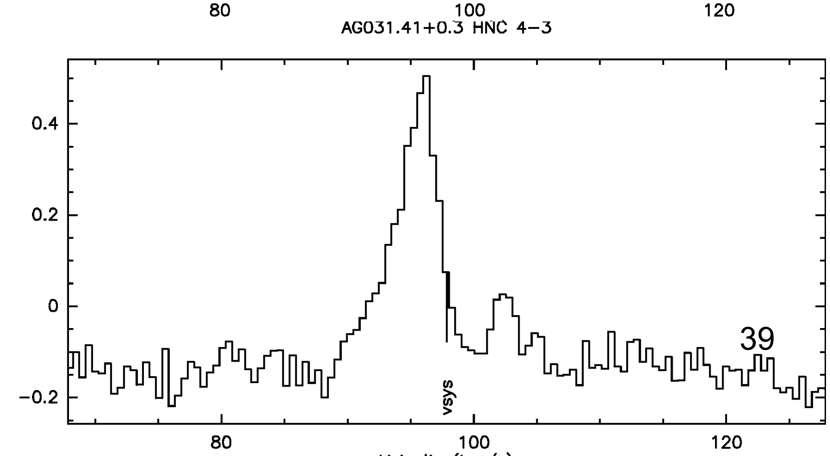

Cycle I: a) continuation to Infrared dark clouds

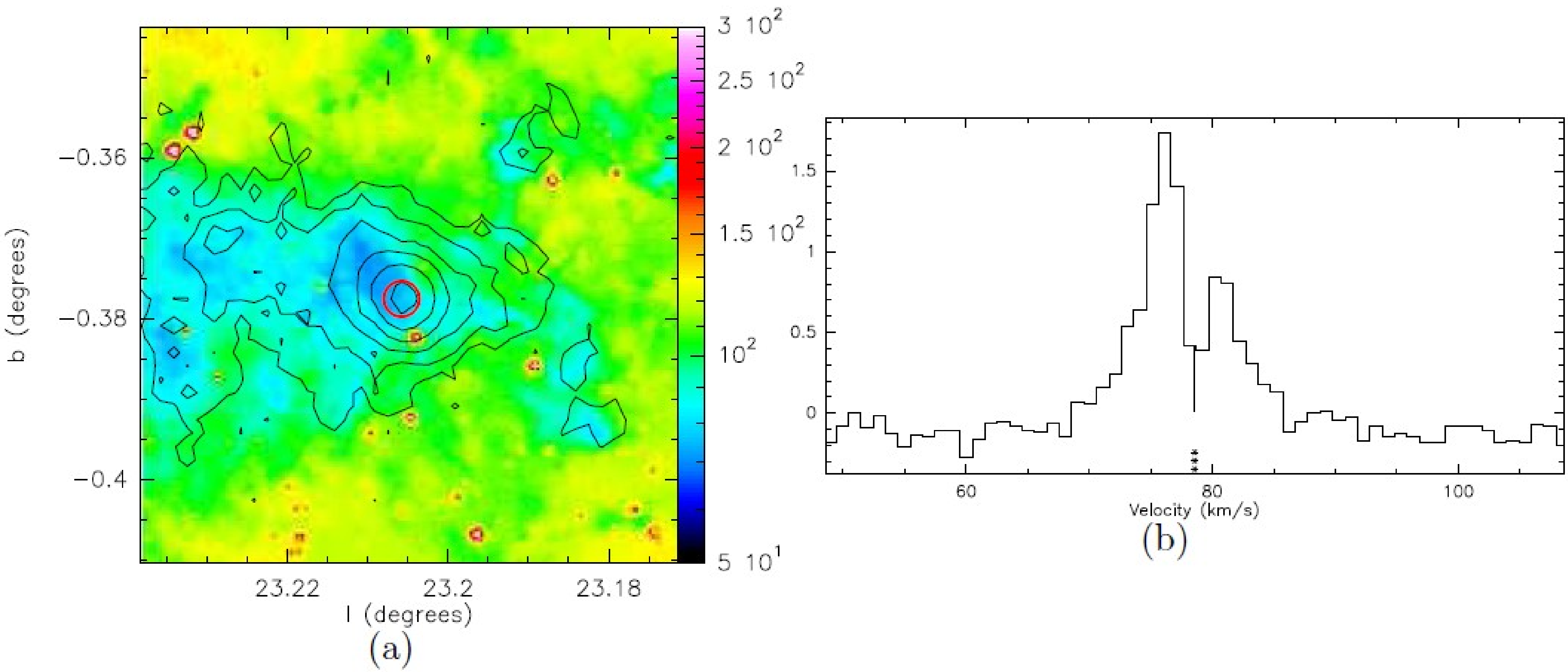

Figure 2: IRDC G23.21-0.38: (a) ATLASGAL 870 μm dust continuum as contours on GLIMPSE 8 μm MIR emission in color, SOFIA beam in red. (b) APEX HNC (4–3) spectrum of this clump with systemic velocity indicated.

Cycle I: b) Filling in further stages:

- G35.20-0.74: submm brightest, northern massive young stellar object, fulfilling Lumsden+ MSX color criteria
- W51E: after SgrB2 brightest northern submm clump, “starburst template”

- → Both again show APEX HNC (4-3) blueskewed profiles

Cycle I: c) Revisit G34.26+0.15

- Improve S/N of absorption:
  - Constrain envelope infall further
  - High velocity infall component close to central object with high ammonia abundance?

Summary

- 3 clear detections of Ammonia line-of-sight infall consistent with results from cm-absorption and/or blue-skewed emission profiles
- More direct probe of infall that can be extended to earlier stages of SF without cm background continuum and cases where other species are depleted
- Infall rates of 3-10 x 10^{-3} $M_{\odot}$/yr (if spherical)
- Future: extend to earlier stages, higher S/N, and possibly further transitions